January 1980

Research on Increased Winter Orographic Precipitation by Cloud Seeding (FY 1980)

Geoffrey E. Hill

RESEARCH ON INCREASED WINTER OROGRAPHIC PRECIPITATION BY CLOUD SEEDING (FY 1980)

DEVELOPMENT OF CLOUD LIQUID WATER INSTRUMENTATION AND APPLICATION TO CLOUD SEEDING TECHNOLOGY

FINAL REPORT

Cooperative Agreement No. 80-5052

July 1979 - June 1980

for the

Division of Water Resources
Empire Building, Suite 300
231 East 400 South
Salt Lake City, Utah 84111

by

Geoffrey E. Hill

December, 1980

UWRL/A-80/01

Utah Water Research Laboratory
Utah State University
Logan, Utah 84322

ABSTRACT

This research continues the development of new instrumentation relevant to the advancement of cloud seeding technology and the analysis of data collected to better understand cloud seeding potential in winter orographic clouds. Instrumentation development included the start of construction of a NOAA type dual frequency radiometer for the continuous measurement of supercooled liquid water and the completion of an expendable balloon-borne system for measuring vertical profiles of supercooled liquid water.

The analysis of data collected on the project was directed primarily at the interpretation of the vertical profiles of supercooled liquid water and vertical motion. Results indicate that sharp vertical gradients of supercooled liquid water often exist in winter orographic clouds. The relationships between measured supercooled liquid water and other variables strongly support previous findings that the precipitation augmentation potential of winter orographic clouds is substantial when the cloud top temperature is -22°C or warmer and the cross-barrier wind speed (at mountaintop levels) is 8 m s^{-1} or greater.

ACKNOWLEDGMENTS

Appreciation is expressed to the University of North Dakota for making several cloud physics flights during periods of other measurements. Appreciation is also expressed for the contributions and participation of the following individuals: Duard Woffinden, electronics engineer; Brad Miller, meteorologist; Martin Miller, meteorologist; and Verl Bindrup, field technician. Section 3.1.2 of this report was written with the assistance of Mr. Woffinden.

TABLE OF CONTENTS

TABLE OF CONTENTS (CONTINUED)

LIST OF FIGURES

LIST OF FIGURES (CONTINUED)

LIST OF TABLES

1.0 INTRODUCTION

1.1 Recent exploratory research at UWRL

To obtain the kind of physical understanding believed necessary to develop a sound as well as efficient seeding technology, a widely based program of inquiry is underway at UWRL. Considerable progress has been made, and our recent progress and plans for the future are presented in this report.

Our recent work has been directed at finding out the detailed sequence of events resulting from the addition of seeding material upwind of a mountain barrier during periods of winter storms. This inquiry includes aspects of the problem such as the transport and diffusion of seeding material, in-cloud effects of seeding as well as the natural distribution and climatology of supercooled water, ice particles and their relationship to other more readily measured parameters such as cloud top temperature. We are interested in finding out the conditions under which supercooled water is found. Such conditions may be related to parameters not so easily measured, such as vertical motion, background ice nuclei concentrations or other factors.

In addition the measurement of precipitation on a space and time scale appropriate to the seeding delivery system and in-cloud responses is required. Furthermore, suitable covariates to precipitation are needed if the natural variability of precipitation is to be partially accounted for.

We believe that the time required in an experiment conducted later to prove a promising hypothesis of seedability could be reduced by a factor of around 3 or 4 by use of suitable covariates.

Thus, the recent research at UWRL represents a marked shift in emphasis from a primarily statistical approach to one stressing physical understanding. Such understanding requires adequate data to verify or modify physical reasoning. In this way, a conceptual framework supported by physical evidence may be developed for the reliable and efficient augmentation of winter snowpack.

1.2 Present directions in research at UWRL

During this past year, research in weather modification of winter orographic clouds was directed along two main lines. One was the development of new instrumentation for measuring critical meteorological parameters relevant to cloud seeding, in particular, for the measurement of supercooled liquid water. The other was the continuation of the measurement of various meteorological parameters during the presence of winter orographic clouds.

The development of two new instruments was undertaken during this year; construction of a dual frequency NOAA type radiometer was in progress, and an expendable balloon-borne sensor for the measurement of vertical profiles of supercooled liquid water was developed.

Measurements made during the winter field season were similar to previous seasons except that supercooled liquid water measurements were also made with the new "cloudsondes." Other measurements included precipitation, vertical motion, rawinsonde data and aircraft measurements of supercooled liquid water and other parameters.

2.0 SUMMARY OF RESEARCH OBJECTIVES AND FINDINGS

2.1 Cloudsonde instrument development

A vibrating wire placed in the humidity duct of a standard U.S. rawinsonde is used to measure vertical profiles of the concentration of supercooled liquid water in clouds. The natural frequency of vibration varies according to the mass of ice accumulated by contact freezing. By monitoring the natural frequency and the airspeed relative to the wire, the supercooled liquid water concentration can be found.

Suitable electronics are developed for both individual expendable rawinsonde units and a ground based receiver so that the vibration frequency can be recorded. Calibration of the frequency change versus mass accumulation is done theoretically along with measurements made in a wind tunnel with supercooled water present. Further verification is found by the use of paint, uniformly sprayed on the "upwind" side of an exposed wire.

Sixteen soundings were made during February and March, 1980. Although no very strong episodes of supercooled clouds were found, some very interesting vertical profiles of supercooled liquid water were measured. These will be discussed in a later section.

2.2 Radiometer instrument development

A dual-frequency radiometer developed recently by NOAA yields continuous readings of vapor and liquid water integrated along a vertical path through the atmosphere. Because of the likelihood of a great benefit to research on winter orographic cloud seeding, it was decided to construct a nearly identical system at UWRL.

It was expected at the outset that the construction of this instrument would take more than one year to complete. In fact, during the first year most of the effort was directed at obtaining components and studying or evaluating system components. (Substantial construction did not actually begin until after this reporting period, but at present only minor tasks remain before the total system is completed.)

2.3 Comparison of J-W and Rosemount supercooled liquid water measurements

Probably the most widely used LWC measuring device is the one described by Neel and Steinmetz (1952) and is generally known as the Johnson-Williams (J-W) hot wire liquid water content meter. At subfreezing temperatures the J-W device measures supercooled liquid water concentrations.

Another device available to measure supercooled LWC is the "Rosemount Ice Detector."[1] The instrument was developed

---

[1]Manufactured by Rosemount, Inc., Minneapolis, Minn. (Our mention of manufacturer does not constitute endorsement.)

in response to a widespread requirement for a reliable aircraft warning system. However, inasmuch as its meteorological use would emphasize the cause of aircraft icing, i.e., supercooled liquid water, identification of the device by the name of Rosemount liquid water (RLW) meter will be used in this report.

The purpose of this phase of our research is to compare supercooled LWC measurements with each of the instruments and to assess their comparative usefulness in cloud physics studies. In particular, our measurements with these instruments were made in winter orographic clouds, but the results should be applicable to supercooled liquid water measurements in general.

The comparison of the Johnson-Williams hot wire device and the Rosemount icing rate meter shows that supercooled liquid water measurements can be made effectively by both instruments subject to certain significant limitations.

The primary well-known limitations of the J-W instrument are the underestimated LWC for droplet sizes exceeding 30 μm and the drift of the zero value, which in winter orographic or cyclonic storms can lead to substantial uncertainty in the readings.

The primary limitations of the Rosemount device are the reduced collection efficiency at droplet sizes less than 10 μm diameter, possible runoff (partial freezing) at warmer temperatures (> -5°C) and aperiodic data gaps due to the brief heating cycle of the instrument.

2.4 Cloud seeding opportunity recognition

One of the main objectives of weather modification research at UWRL is to develop improved seeding criteria for precipitation augmentation of winter orographic clouds. In this study detailed measurements of supercooled cloud water, precipitation, cloud top temperature and vertical air motion in winter orographic clouds are used to develop criteria for the seedability of those clouds. Winter orographic clouds over the upwind mountain base with cloud top temperatures between 0°C and -22°C are found to be primarily composed of supercooled water and are therefore seedable. The supercooled water concentration is empirically found to depend upon the updraft velocity. The potential precipitation yield is dependent upon the flux of supercooled water over the barrier. Because the updraft velocity is approximately proportional to the cross-barrier wind, the potential precipitation yield is approximately proportional to the square of the cross-barrier wind, provided that the cloud top temperature is in the seedable range of temperatures.

These findings are strongly substantiated by systematic use of aircraft icing reports over a full winter season (November-March, 1978-79). It is shown that a cloud top temperature of about -22°C separates clouds with a precipitation enhancement potential from those without such a potential. It is found that aircraft icing is approximately proportional to the cross-barrier wind, and that the flux of supercooled water over the barrier for cloud top temperatures warmer than -22°C is (as derived from the research data) approximately proportional to the square of the cross-barrier wind.

About 20 percent of cloud episodes over the mountains of Northern Utah may be expected to have a high modification potential.

3.0 DEVELOPMENT OF EQUIPMENT

3.1 Cloudsonde instrument

3.1.1 Concept. The basic concept utilized for measuring supercooled liquid water concentration (SLWC) is a vibrating wire exposed to the airstream during ascent of a balloon-borne package. The wire is fixed at one end and free at the other as indicated schematically on Fig. 1. The package consists of a standard NWS rawinsonde, modified to accommodate the vibrating wire and related electronics. The natural frequency of vibration varies according to the mass of ice accumulated by contact freezing. Thus, by monitoring the rate of change of the natural frequency and the airspeed relative to the wire, the supercooled liquid water concentration can be determined.

In selecting a suitable ice collector, an important consideration is the collection efficiency. It is desirable to choose a collector of sufficiently small diameter so that the collection efficiency does not vary much for the drop sizes encountered. Collection efficiencies for various drop sizes and collector diameters were calculated according to Langmuir and Blodgett (1946). Based upon these calculations, a (piano) wire of 0.60 mm diameter was chosen. Slightly smaller diameters would have been acceptable but the stiffness and vibration properties were not as suitable as the value chosen. The length of the wire was set at 90 mm, so

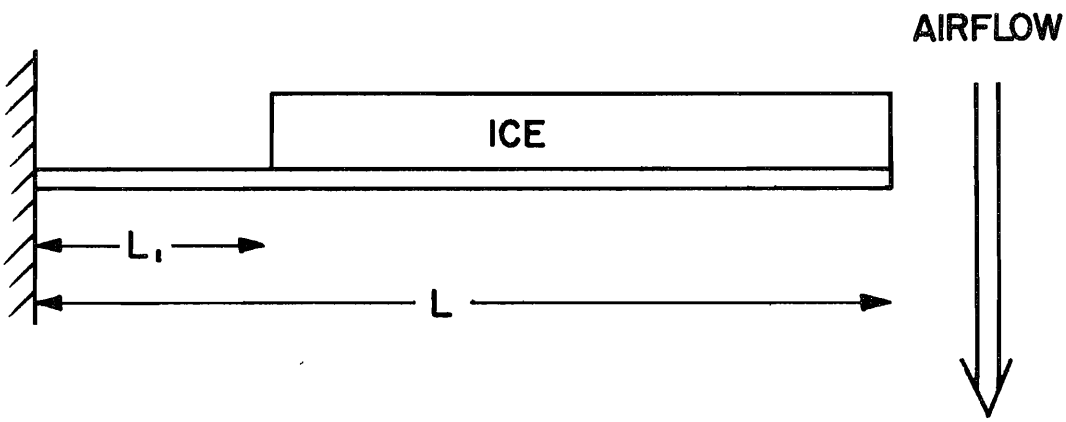

Fig. 1. Illustration of ice-loaded wire.

the natural vibration frequency is around 53 Hz. The collection efficiencies for the wire as a function of droplet size with an airspeed of 5 m s^{-1} approach unity above droplet sizes of about 10 μm. Because the bulk of SLWC is expected to be found with diameters in excess of 10 μm a correction factor of a few percent could be added to the measurements to compensate for slightly reduced efficiencies from unity.

In interpreting the droplet collection efficiencies we may expect that supercooled water will be underestimated when the predominant droplet diameters are less than about 10 μm. Such conditions might be found in heavily polluted continental clouds. Problems with collection of larger droplets such as encountered with the Johnson-Williams (J-W) device would not be expected with the vibrating wire. When large supercooled water droplets impinge on the J-W hot wire not all of the droplet contributes to cooling because heated droplets flow past the wire. With a relatively slow airflow past the vibrating wire and no heating externally applied, we may expect little problem in measuring supercooled water at large cloud droplet sizes.

In addition to the collection efficiency, consideration must also be given to the heat economy of the collecting wire for reasons discussed by Ludlam (1951) and others.[2] In

---

[2]For example, see Brun, R. J., W. Lewis, P. J. Perkins, and S. J. Serafini, 1955: Impingement of cloud droplets on a cylinder and procedure for measuring liquid-water content and droplet sizes in supercooled clouds by rotating multi-cylinder method. N.A.C.A. Report No. 1215. 43 pp.

exposed cylinders mounted on aircraft, there is a temperature dependent limit of supercooled water concentration beyond which there is very little additional rate of accumulation. While such limits exist for a balloon-borne vibrating wire, the critical concentrations are far above the concentrations expected in the atmosphere except at temperatures within a degree below freezing. The reason for the very limited below-freezing temperature range where incomplete freezing takes places is that both the airstream velocity and the probe diameter are much lower than in the case of aircraft.

3.1.2 Mechanical/electronic design. The design of SLWC measuring system consists of two parts: the balloon-borne package and the ground based rawinsonde (R/S) receiver-recording system. In the balloon-borne package the SLWC signal is generated by the vibrating wire which is driven by a coil mounted on the outside of the humidity duct. The vibrating wire extends from the driving coil into the humidity duct; 65 mm of the 90 mm wire are exposed to the airflow. A very small pickup coil is mounted near the free end of the wire; the pickup coil serves to feed back the natural frequency so the drive coil acts at the natural frequency, which is allowed to vary. As indicated in Fig. 2 the signal from the driving oscillator is fed into a Schmidt trigger and a monostable multivibrator to eliminate noise and enhance the signal. Then the signal is fed into a phase-locked loop and the frequency is multiplied by ten. The multiplication by

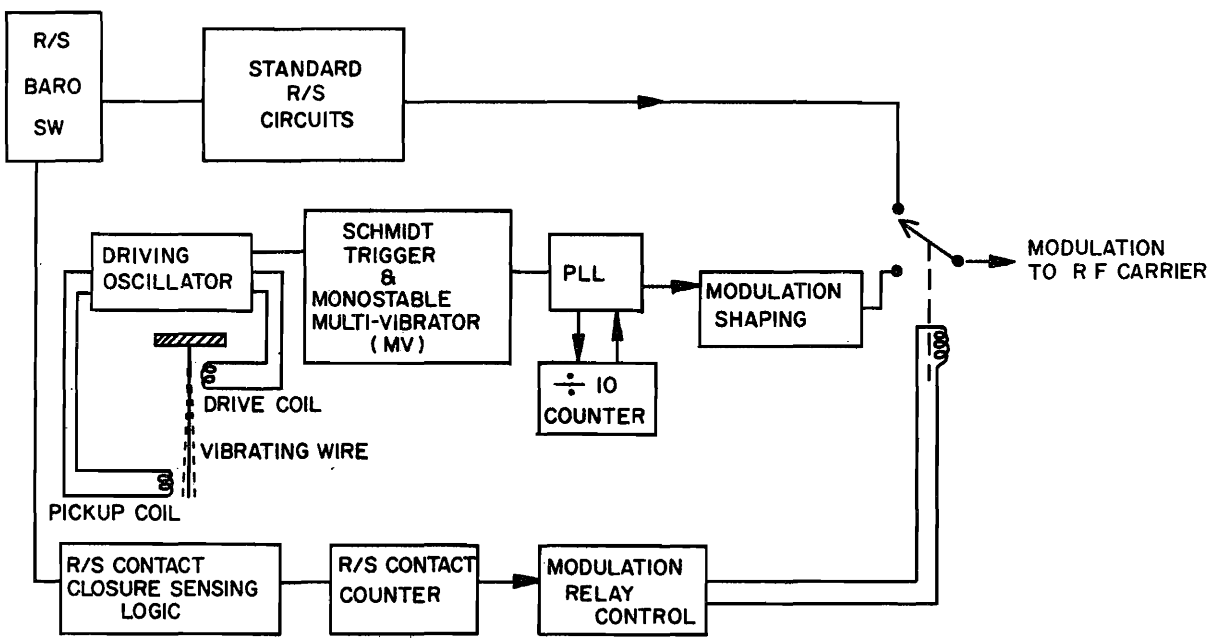

Fig. 2. Block diagram of modified rawinsonde for measurement of SLWC.

ten not only separates the received signal from other parameters, but amplifies the response to collected ice prior to transmission. After multiplication the signal is passed through a modulation shaping circuit to properly modulate the radio frequency (rf) carrier.

The remaining circuits act to intersperse the liquid water measurements in place of alternate temperature samples. This is done by sensing each baroswitch closure and actuating the modulation control relay just after every other closure. Each closure represents either humidity, low reference or high reference and, because a temperature sample normally follows each, it is necessary to sense and count all three types of closures so the liquid water samples can be adequately monitored.[3]

The signal output from the RD65CS receiver is a series of narrow pulses occurring at the frequency of the modulation on the radiosonde transmitter carrier. This signal frequency is 0-200 Hz for a standard R/S, but when driven by the SLWC sensor it is 470-550 Hz. A block diagram of the modified R/S-receiver circuits is shown in Fig. 3. The pulses representing SLWC are quite narrow and are therefore unsuitable for the frequency-to-voltage (F/V) converter which requires a duty cycle of at least 20 percent for frequencies below 1

---

[3]Modification of circuits is made for newer type rawinsonde units; in this case FM modulation allows for continuous transmission of supercooled water information.

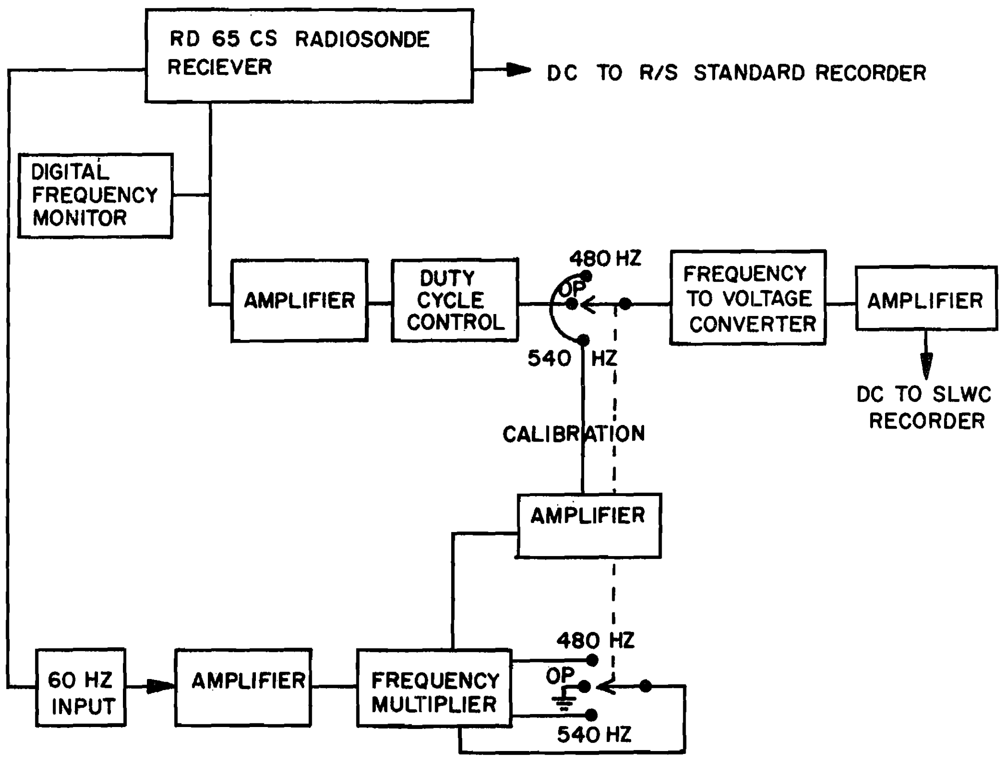

Fig. 3. Block diagram of modified rawinsonde receiver for obtaining SLWC data.

kHz. Therefore, the pulses are stretched so that their duty cycle is from 45 to 55 percent. The output of the F/V converter is amplified and recorded on a strip-chart recorder. The deflection on the recorder is approximately proportional to the mass of ice accumulated by the sensor.

Calibration of the recorder is achieved by inserting first a 480 Hz signal and then a 540 Hz signal. These two frequencies define a range which represents 60 cycles of frequency change. Thus, the chart is calibrated in terms of chart divisions per cycle.

Calibration of the ice load and consequent change in vibration frequency in terms of liquid water concentration is given in detail by Hill and Woffinden (1980).

3.1.3 Application. During February and March, 1980 16 vertical profiles of supercooled liquid water concentrations were made using cloudsonde instruments. For a detailed example, the test case of February 7, 1980 will be described as follows:

At 1710 MST on February 7, 1980 a strato-cumulus deck estimated to be at about 1400 m elevation above ground was over Richmond, Utah (elev. 1386 m), the launch site for SLWC soundings. At that time a launch was made; the measured temperature and dew point are shown in Fig. 4. No evidence of precipitation could be seen falling from the clouds. As indicated by the temperature dew-point profiles, the strato-cumulus deck was the result of mixing at lower levels.

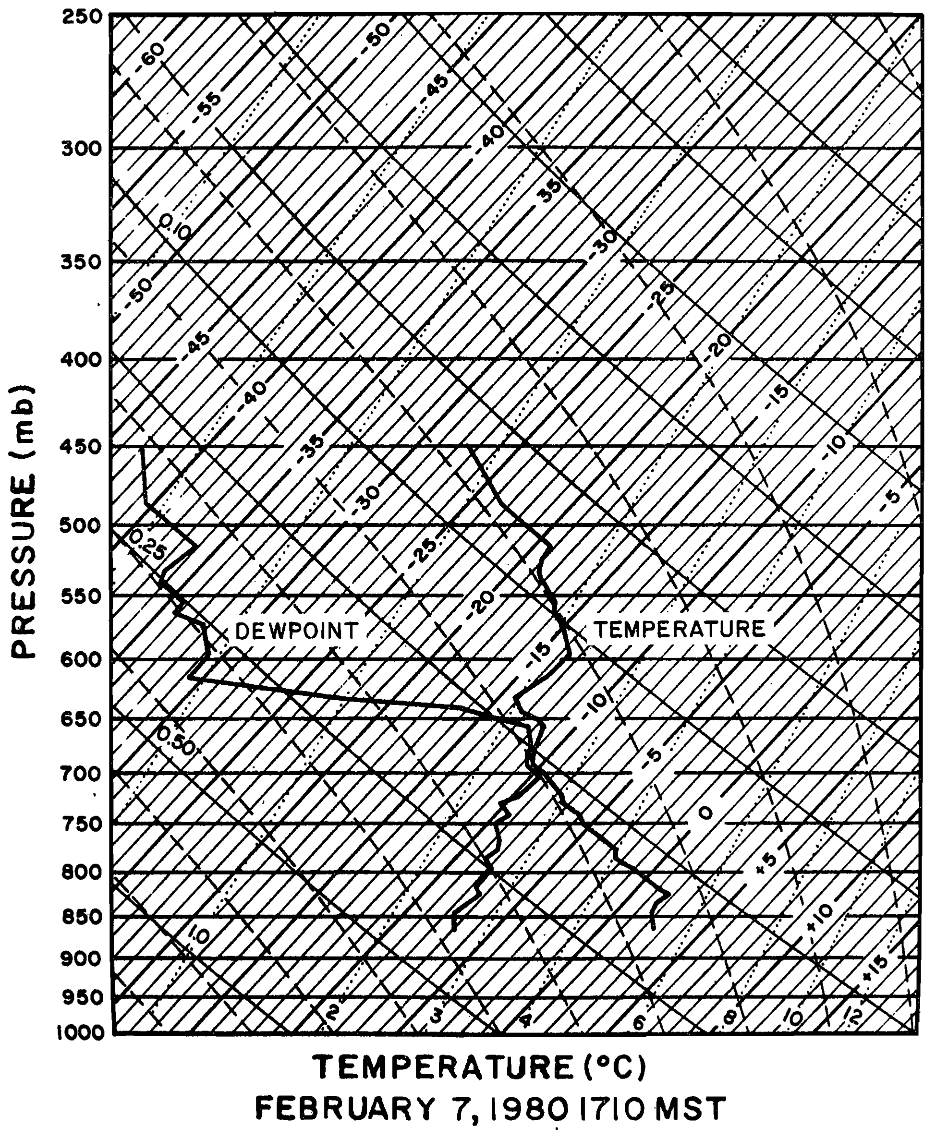

Fig. 4. Skew-T diagram of temperature and dew point for February 7, 1980 at 1710 MST.

Adiabatic values of liquid water would not be expected to exceed 0.3 g m^{-3}. In fact, due to mixing the actual SLWC would be expected to be somewhat lower.

In this example no vertical motion sample was made. However, for our present purpose, the balloon-rise rate below cloud level is used for the airflow velocity and the vertical air motion is assumed zero. Therefore, we set $w = 4.6$ m s^{-1}. Values of the vibration-frequency as transmitted (f') and the time between samples are listed in Table 1 as a function of height.

The presence of supercooled liquid water is identified by the negative values of frequency change ($\Delta f'$). The

Table 1. Change in vibration frequency versus height and time.

Mid-layer Height (m)	Δt (s)	Top-of-layer f' (Hz)	$\Delta f'$ (Hz)
1644	42.0	544.0	-
1838	32.1	544.0	0.0
2034	42.6	544.1	0.1
2228	41.7	544.1	0.0
2426	32.7	544.2	0.1
2626	48.3	544.2	0.0
2824	44.1	544.3	0.1
3026	53.4	544.3	0.0
3228	43.2	543.0	-1.3
3432	48.9	541.1	-1.9
3580	47.0	541.3	0.2
3690	54.3	543.8	2.5
3845	74.4	544.2	0.4
4005	39.0	544.8	0.6
4160	28.0	544.8	0.0

relatively strong positive changes in f' above the cloud layer are due to sublimation. The amount of sublimation depends upon prior ice accumulation and the relative humidity of the ambient air. In this case the air above the cloud was very dry as shown in the sounding. In addition to these variations in f' there is a very small temperature effect (0.053 Hz per °C reduction).

According to the measured frequency changes, the SLWC is 0.10 g m^{-3} over a 204 m layer (694-676 mb) centered at 3228 m and 0.13 g m^{-3} over a 205 m layer (676-658 mb) centered at 3432 m. Thus, the cloud thickness as determined by SLWC measurements is no more than 409 m, probably about 350 m, and the supercooled liquid water concentration is in the vicinity of a tenth g m^{-3}.

Other soundings recently made show examples of much larger amounts of supercooled water and others show a virtual absence of supercooled water, especially in the presence of snowfall. These will be described in Section 5.2.

3.2 Radiometer instrument

To obtain continuous measurements of supercooled liquid water the construction of a NOAA type dual frequency radiometer was undertaken. This radiometer is nearly identical to the one developed by Guiraud et al. (1979). The two frequencies are 20.6 GHz and 31.6 GHz. One specially designed horn antenna (NOAA) is used. A flat reflector outside and an offset parabolic reflector inside cause cloud water and vapor radiation to enter the horn antenna, whereupon the two frequencies follow separate wave guides. Two Dicke switches then alternate between "reference" or cold load, a "hot" load, and the data signal. With this information for each frequency the radiation amount at the two frequencies is found. An HP-85 computer in the trailer unit is used to perform the various calculations required to obtain the vertically integrated vapor and liquid amounts. The HP-85 has on-board capability for graphics, printing, and magnetic data tape storage. It is noted that in the mobile trailer extendable beams are available for mounting the flat reflector--which itself weighs 50 kg.

During the year most of the components were ordered; many required six months or more for delivery. However, by the end of the project year, all but a few components were on hand. Little actual construction was accomplished during the year. On the other hand at the time of this report, the radiometer was near completion, as shown in Figs. 5 through 8.

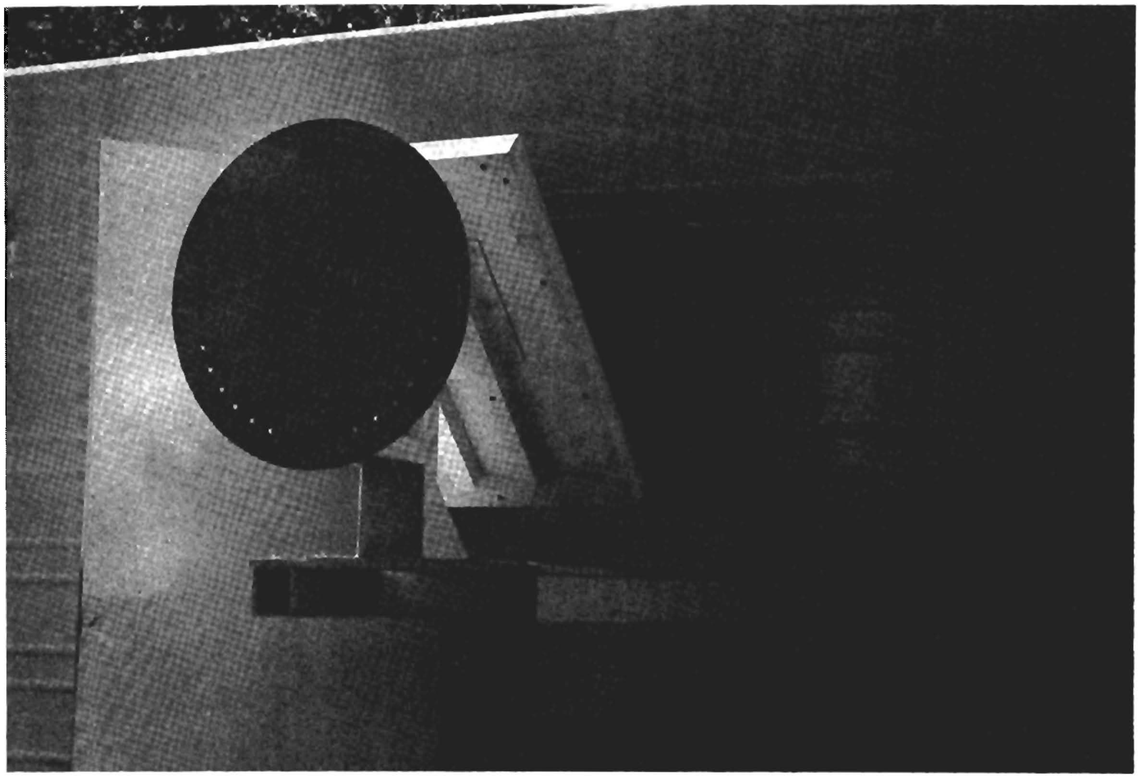

Fig. 5. Radiometer outside reflector.

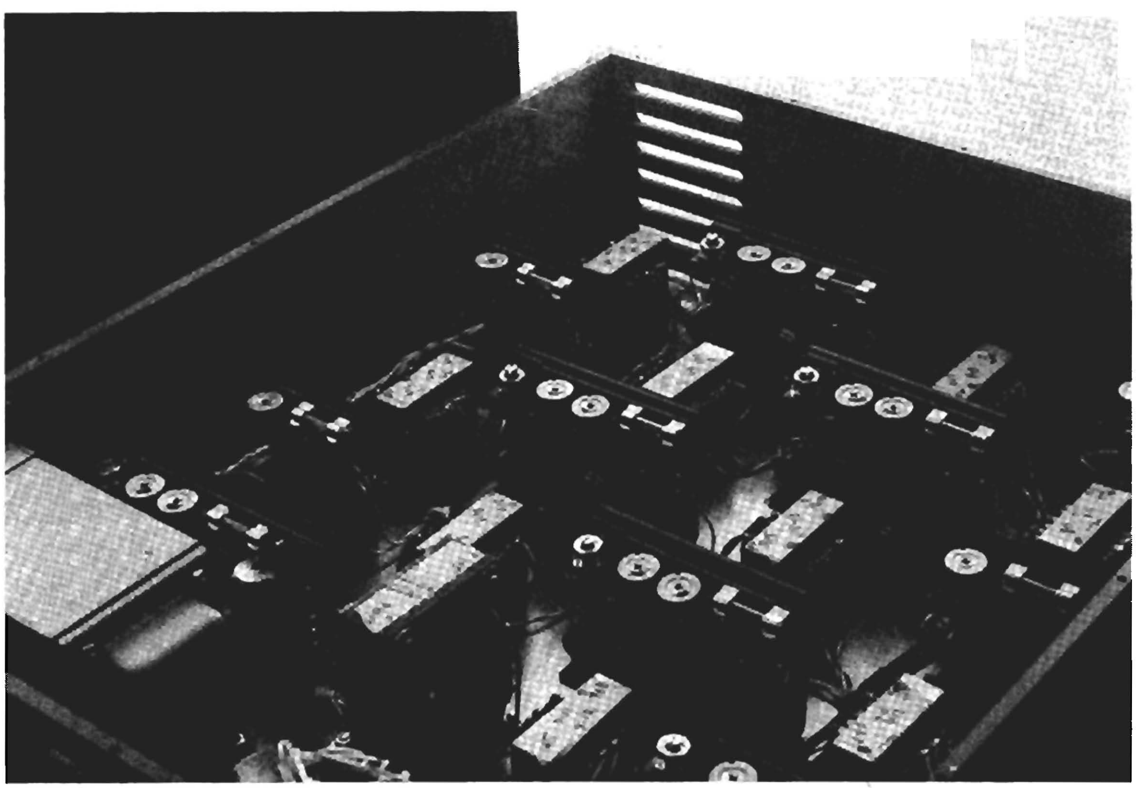

Fig. 6. Radiometer power supply.

Fig. 7. Radiometer antenna and electronics.

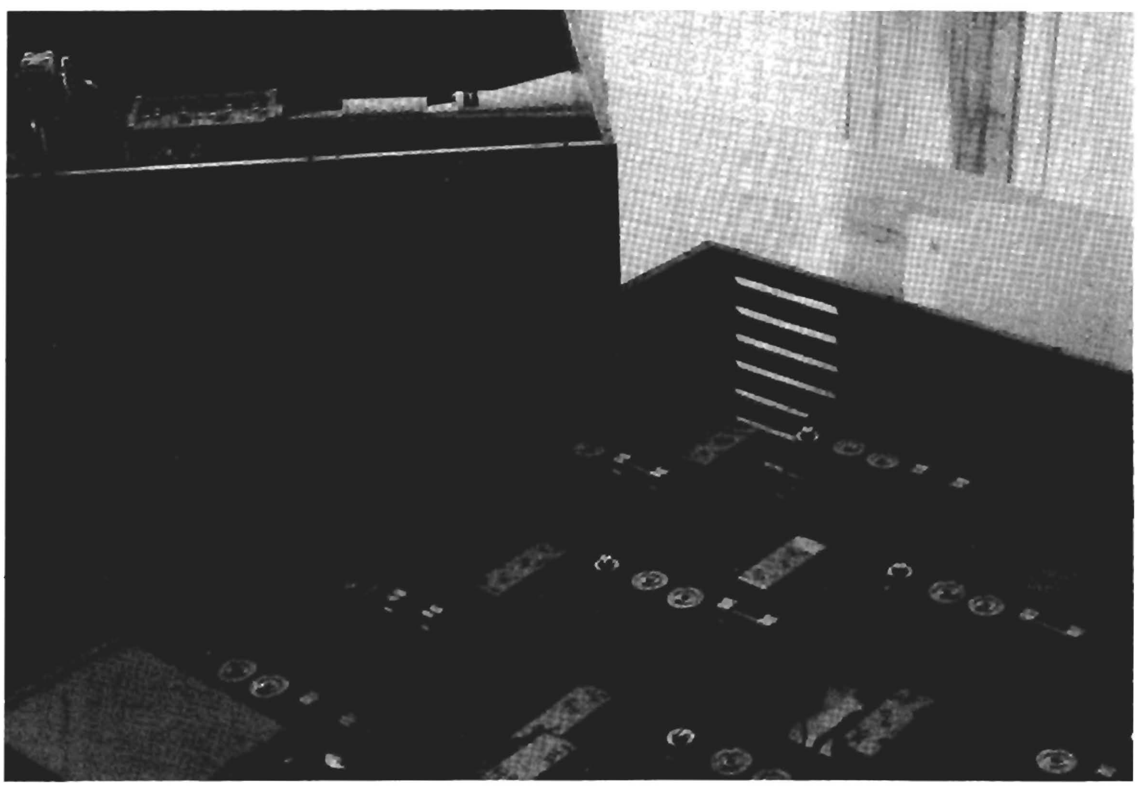

Fig. 8. Radiometer power supply, antenna and electronics.

4.0 DATA ACQUISITION AND OPERATIONS

During the 1979-80 winter season no seeding was planned. Emphasis was placed upon making liquid water measurements and determining seedability rather than attempting to find seeding effects. This choice was made because it has been found in our research that airborne released silver iodide generally does not mix very much within a period of an hour or so after release. On the other hand our previous data indicated that seedability could be identified by cloud top temperature and the cross-barrier wind speed. Therefore, the field research undertaken in the 1979-80 winter season was directed toward obtaining data related to seedability.

During February and March eight periods (events) of special study were used for making surface and upper level measurements when winter orographic clouds were present. The length of the events varied because of the many technical problems encountered in the first operational use of the USU cloudsondes.

4.1 Precipitation

Precipitation measurements were made over the period from mid January through the end of March, 1980. The layout of the precipitation network for the 1979-80 winter season is shown in Fig. 9. Precipitation at Smithfield Canyon is shown in Fig. 10 along with the periods of field operations. Further analysis of these data will be described in Section 5.

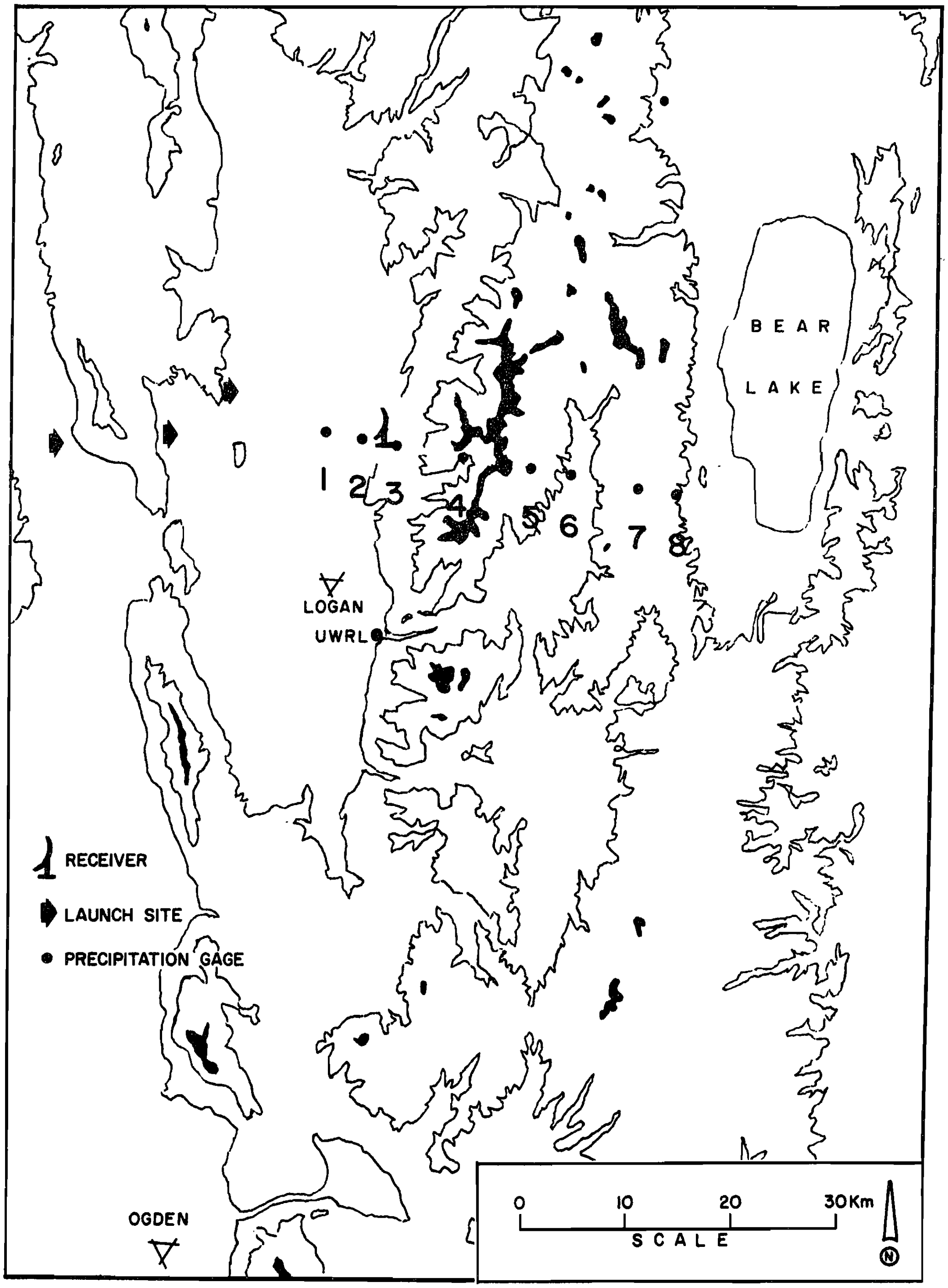

Fig. 9. Precipitation network, FY80.

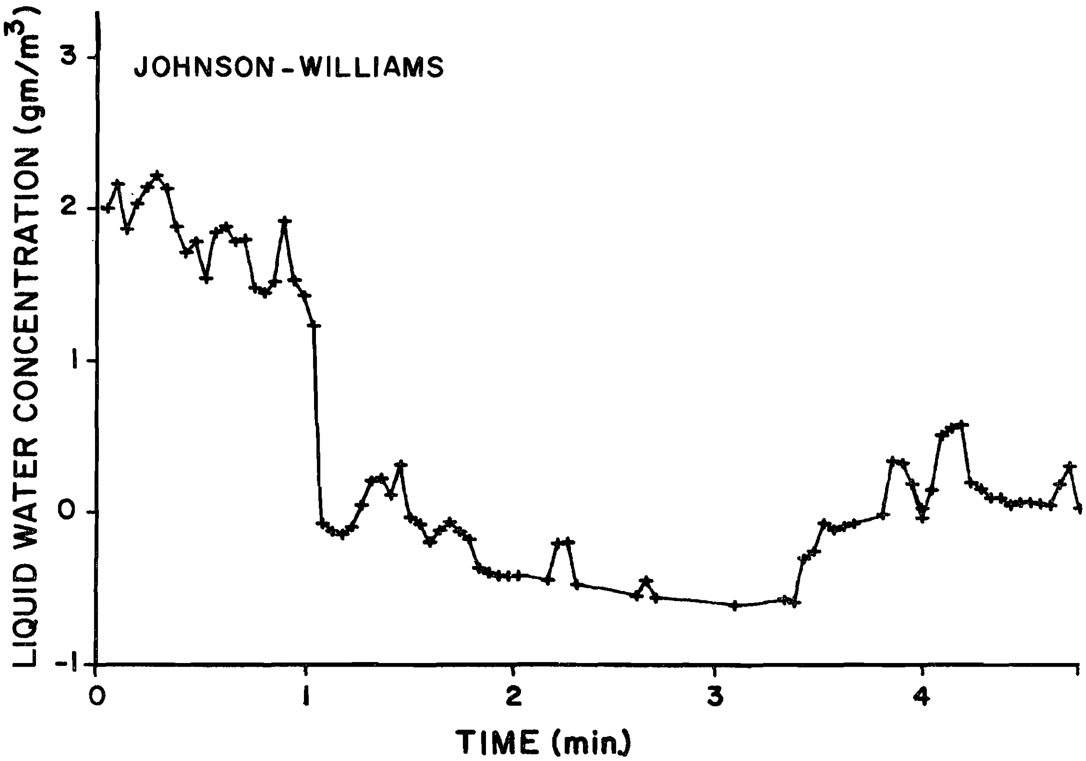

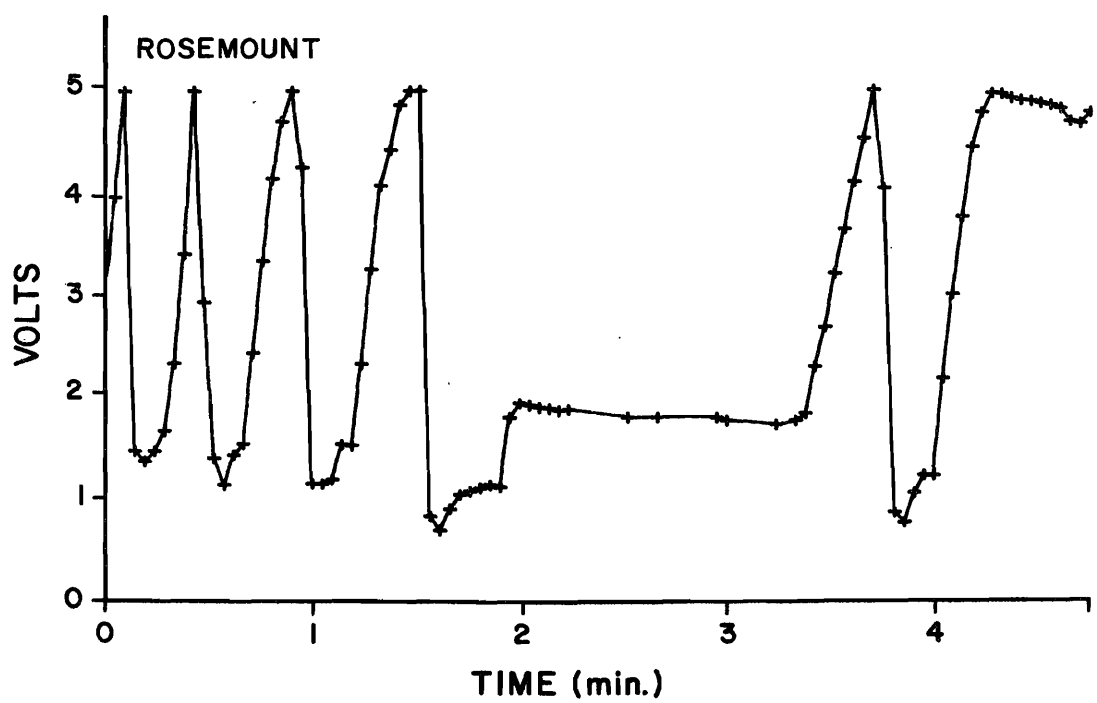

Fig. 10. Sample liquid water raw data for Johnson-Williams vs Rosemount devices with moderate concentration of liquid water.

4.2 Airborne cloud physics measurements

As part of the research effort aircraft measurements were made during four of the eight events. The aircraft operated by the University of North Dakota was used in the research. Measurements were made of supercooled liquid water, ice particle concentration, temperature, and various parameters concerning aircraft operation, including time, VOR, DME, rate of climb, airspeed, and altitude. The flight track of the aircraft was directly over the precipitation network at an altitude of 13,000 ft.

4.3 Upper level soundings

During each of the eight events upper-level soundings were made to obtain data on cloud structure, airflow, and stability. The soundings included the use of the vibrating wire system for finding liquid water concentration. In addition, other soundings were made to obtain vertical motion.

To summarize the operations during FY80 a list of events according to date and time along with the parameters measured is given in Table 2. In addition several test soundings for SLWC were made in February and March, 1980. Of particular interest in these data are the vertical profiles of vertical motion and liquid water. Analysis of these data will be discussed in Section 5.

Table 2. List of events according to date and time along with parameters measured.

1980 Event No.	Date	Time (MST)	Airborne Measurements	Rawinsonde	Vertical Motion	SLWC
1	Feb. 15	1600-1800	✓	1	1	1
2	Feb. 17	1230-1700	✓	3	3	3
3	Feb. 18	1200-1530	✓	2	2	2
4	Feb. 19	1600-2130	X	3	3	3
5	Feb. 21	1700-2100	X	3	2	1
6	Mar. 3	1200-2200	X	5	3	4
7	Mar. 5	1300-1930	✓	4	4	3
8	Mar. 11	2000-2200	X	2	0	2

✓ indicates measurements were made: X indicates measurements were not made. Numbers in last three columns indicate number of soundings.

5.0 DEVELOPMENT OF CLOUD SEEDING TECHNOLOGY

5.1 Airborne measurements of supercooled liquid water

5.1.1 Comparison of J-W and RLW measurement of supercooled liquid water. During water years 1978 and 1979, 20 flights over the Northern Wasatch Mountains were made when orographic clouds were present. In several cases the liquid water concentration was essentially zero, or at least below the level of detectability. In other cases the J-W device was not operating properly. On the other hand the Rosemount device operated without trouble. Of the remaining cases with both significant concentrations of supercooled liquid water and the two instruments operative, data were available from 3 cases in 1978 and 3 in 1979.

Before comparing these six cases it is useful to display samples for each measuring device. In Fig. 10 the J-W and Rosemount output every 2.8 s is shown for a moderate concentration of LWC and in Fig. 11 for a heavy concentration. The J-W values are read directly in g m^{-3}; the Rosemount values are proportional to the average ice thickness on the probe and conversion is needed to express in an LWC concentration.

From inspection of the Rosemount output it is clear that the heating cycle obscures the measurements part of the time. The assumption made herein is that heating effects are completely absent between a level of 2.25 V and 4.50 V.

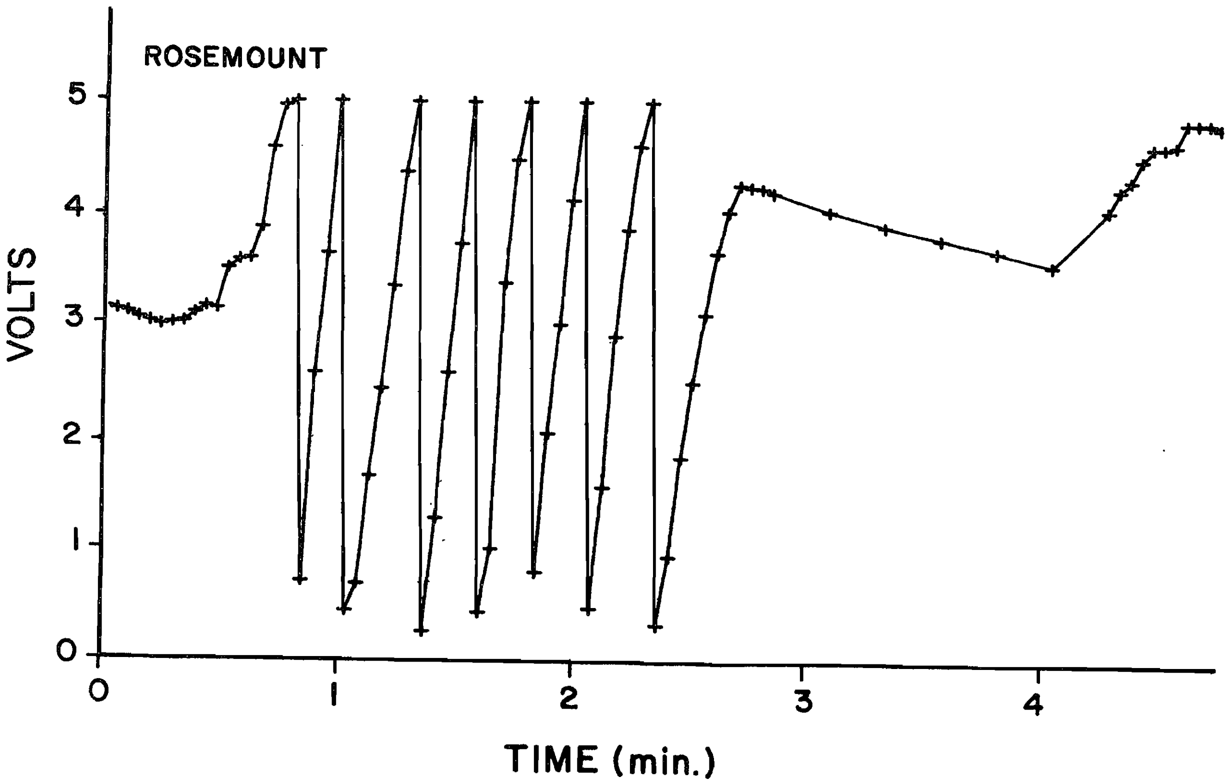

Fig. 12. Sample output of Rosemount device in and out of cloud.

altitudinal effects on the J-W measurements not fully eliminated by the instrument design.

The results of the foregoing analysis are depicted for a composite of all events in Fig. 13; paired values of J-W and Rosemount LWC are plotted in the figure. The overall correlation coefficient is 0.85 with 148 observations. The mean concentration is 0.61 g m^{-3} for the Rosemount and 0.60 g m^{-3} for the J-W.

5.1.2 Evaluation of the instruments. In all events some of the scatter is attributable to differences in the way the data are recorded. Whereas the Rosemount data are integrated between readings on account of an ice accumulation, the J-W data are instantaneous values determined by the rates of cooling due to the liquid water. In very high LWC this difference causes increased scatter between readings of the two devices.

It is noted that higher scatter occurs with rapidly varying concentrations. This is due in part to the slight offset in recording times. The Rosemount readings were recorded about 1.4 s after the J-W readings. With typical time intervals of only 5 or 6 s between a Rosemount reading of 2.25 and 4.50 volts in the case of high LWC, some additional error is introduced in the comparison.

However, overall there is general agreement between the two measurements as indicated by the correlation. While the J-W device has received wide usage, the Rosemount device has

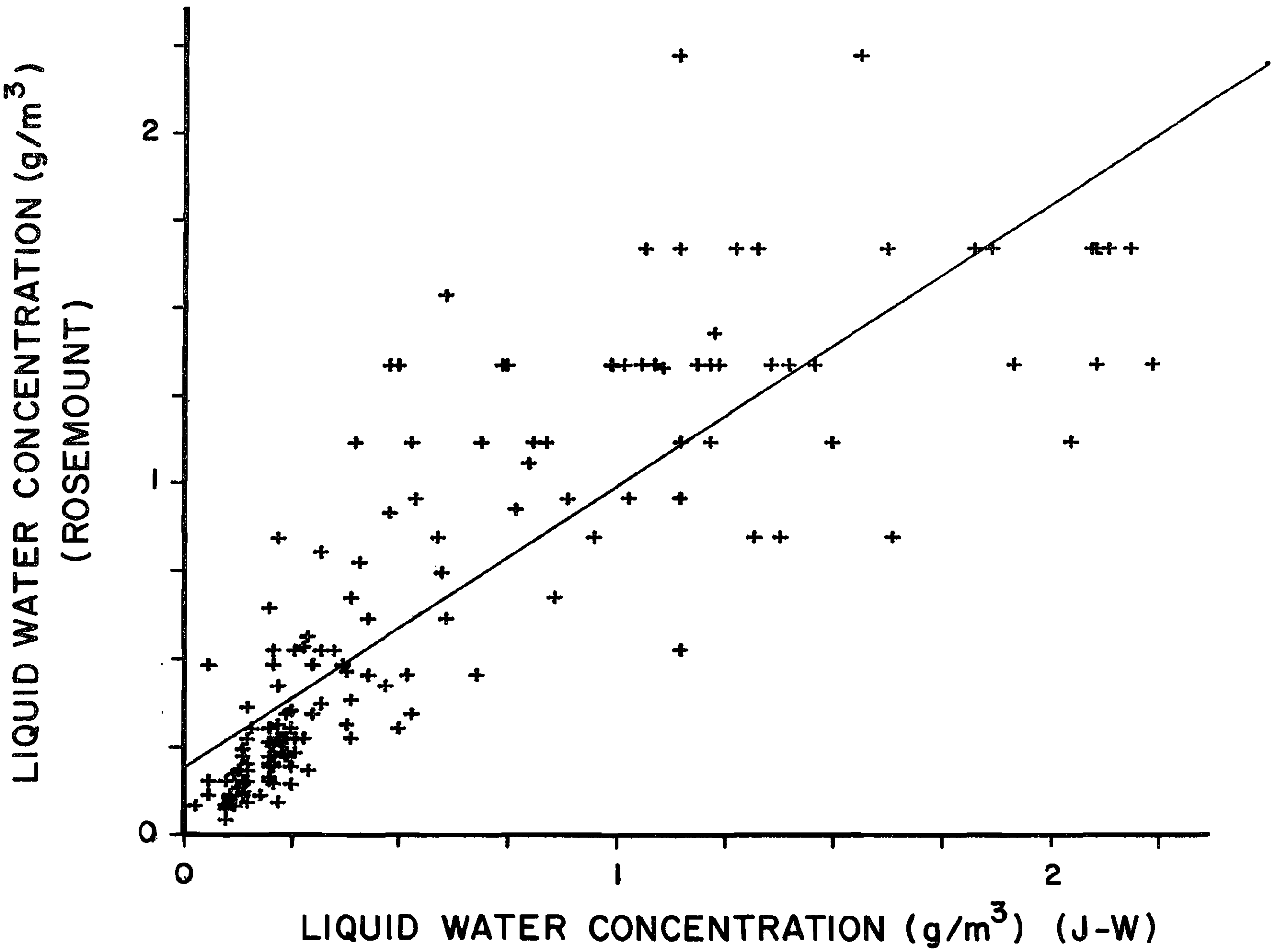

Fig. 13. Liquid water concentrations measured by Johnson-Williams and Rosemount devices for 6 events in FY78 and 79.

certain advantages: there is no discernible "zero drift," out-of-cloud periods are clearly identifiable, the instrument appears to have a higher degree of operational reliability and the liquid water concentrations are integrated over the measurement interval (2.8 s in the present instance) rather than the instantaneous values given by the J-W device.

5.2 Cloudsonde measurements

5.2.1 Standard measurements. During February and March, 1980 measurements of temperature, humidity, wind and pressure/height were obtained from both the cloudsonde (SLWC) and vertical motion soundings. Of particular importance are rawinsonde derived cloud top temperatures and cross-barrier wind speeds. Discussion of these data will be interspersed with other aspects of the measurement program in the sections to follow.

5.2.2 Vertical profiles of supercooled liquid water. As an example of data collected during the winter (1979-80) the vertical profile of temperature and humidity are shown in Fig. 14 for March 12, 1980, 1140 MST. The concurrent profile of supercooled liquid water is shown in Fig. 15.

It is noted that the highest SLWC is near the top of the cloud. The cloud top temperature is around -23°C. Precipitation over the barrier is restricted to the downwind side of the barrier with rates of less than 0.25 mm h^{-1} (0.01 in h^{-1}).

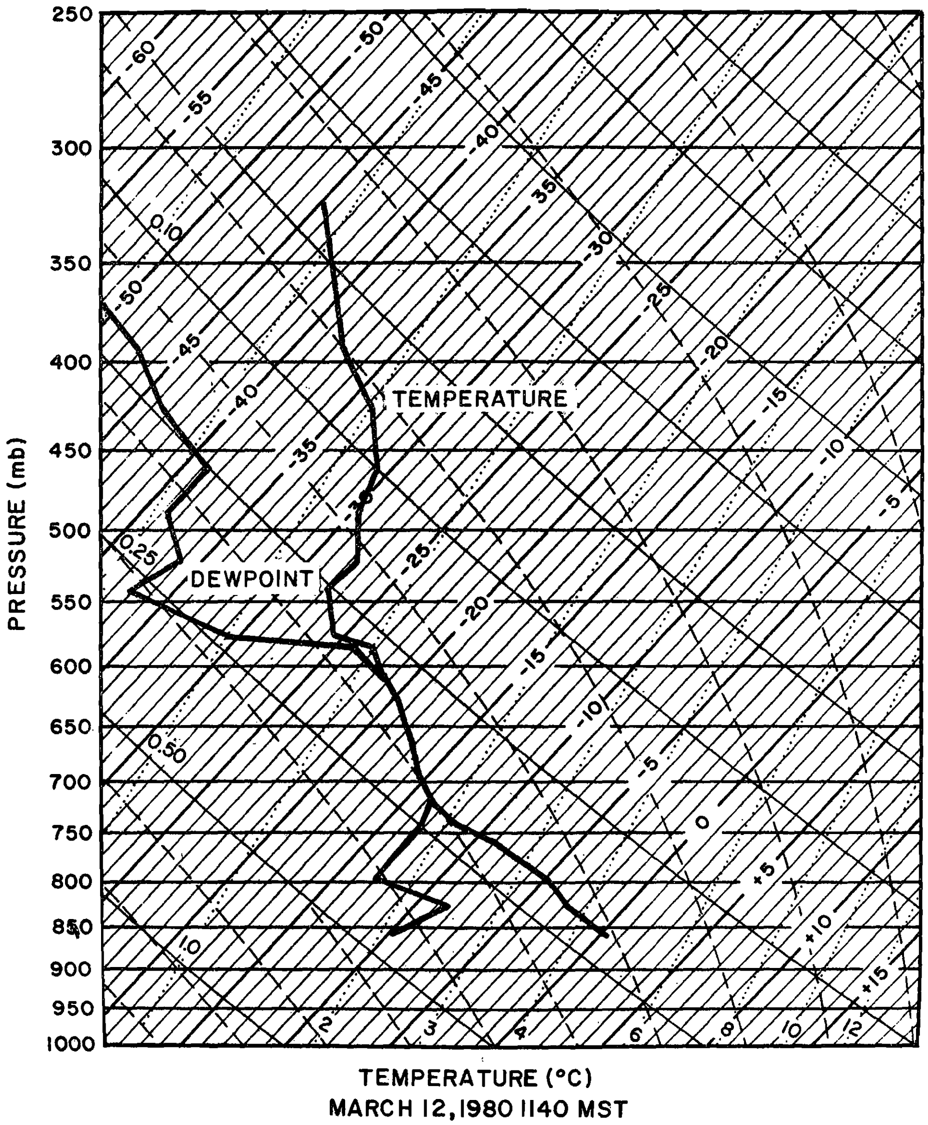

Fig. 14. Skew-T diagram of temperature and dew point for March 12, 1980, 1140 MST.

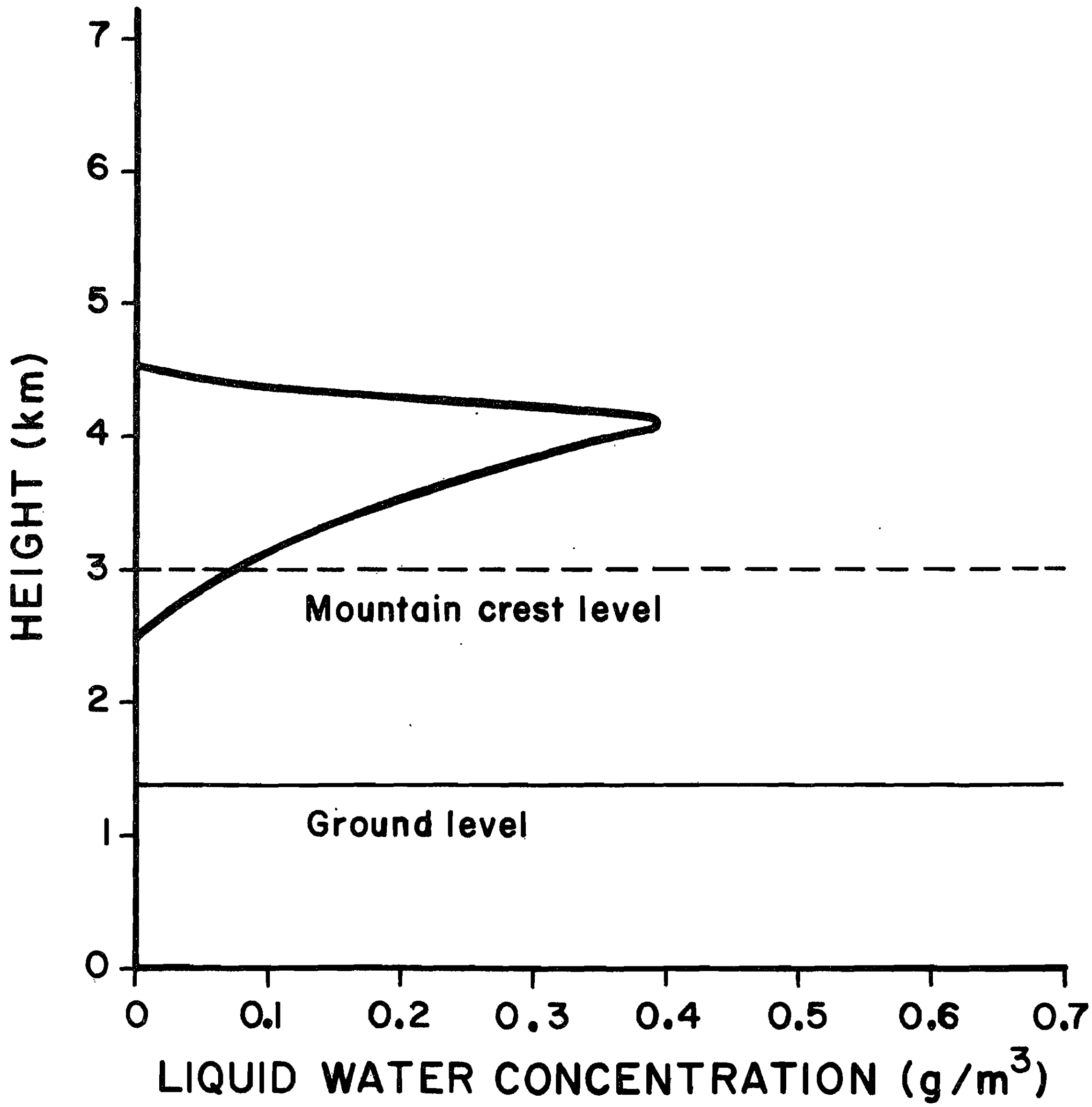

Fig. 15. Vertical profile of supercooled liquid water for March 12, 1980, 1140 MST.

With an airflow over the barrier of about 8 m s^{-1}, a calculated flux of liquid water is approximately 0.2 g m^{-3} x 1,500 m x 8 m s^{-1} = 2,400 g m^{-1} s^{-1} = 7.2 x 10^6 g m^{-1} hr^{-1} = 7.2 x 10^4 g cm^{-1} hr^{-1}. If all this amount were spread as precipitation over 10 km, then the depth of water would be 0.72 mm in an hour. Compared to the observed precipitation only a small fraction of the condensed water was precipitated, and this was on the far side of the barrier.

Had these conditions prevailed for 24 hrs the precipitation potential would have been 1.73 cm (0.692 in). This would constitute a very substantial amount of added water. There is in fact some evidence that these conditions were present the day before according to two soundings (March 11, 1980, 2030 MST and 2130 MST).

Thus, it is shown that supercooled liquid water measurements such as described here can be very useful in identifying clouds which could yield increased precipitation by cloud seeding. Just how seeding material is to be effectively dispersed into a cloud is another problem, not addressed here.

Finally, it is noted that all other instances of measured supercooled water occurred in layers of saturated air but not in subcloud regions wherein precipitation sometimes occurred. In other words, the supercooled liquid water measuring device distinguishes between SLWC and precipitation. A summary of data obtained by these measurements is given in Table 3. Analysis of these data will be presented in Section 5.3.5.

Table 3. FY80 cloudsonde and precipitation data.

Date	Time (MST)	Cloud Base Temperature (°C)	Cloud Top Temperature (°C)	Maximum SLWC (g m^{-3})	Hourly* Precipitation (cm h^{-1})	Cross-Barrier Wind** (m s^{-1})	Convection
Feb. 15	1815	-10	-11	0.02	0.00	7	
Feb. 17	1355	-1	-27	0.10	0.06	15	
Feb. 17	1535	0	-18	0.20	0.01	12	
Feb. 17	1745	-2	-17	0.15	0.02	12	
Feb. 18	1337	-8	-19	0.20	0.00	9	
Feb. 18	1500	-11	-13	0.03	0.005	4	
Feb. 19	1930	-3	-14	0.15	0.01	2	
Feb. 19	2115	-2	-5	0.03	0.01	1	
Feb. 21	2040	-13	-15	0.25	0.03	4	
Feb. 23	1445	-3	-24	0.35	0.04	4	CB Overhead
Mar. 3	1810	0	-51	0.06	0.30	10	
Mar. 5	1355	-5	-36	0.15	0.05	3	
Mar. 5	1835	+1	-13	0.30	0.64	16	Thunderstorm
Mar. 11	2030	-2	-13	0.55	0.26	6	CB (T at SLC)
Mar. 11	2130	-8	-17	0.35	0.22	10	CB (T at SLC)
Mar. 12	1140	-14	-22	0.40	0.00	8	

*At Smithfield Canyon.

**At 2700 m (9000 ft).

5.3 Analysis of seedability

5.3.1 Cloud modification potential. To assess the modification potential of a cloud we first define precipitation efficiency, ε, as

$$\varepsilon = P/C \quad . \; . \; . \; . \; . \; . \; . \; . \; . \; . \; . \; . \quad (1)$$

where P and C are the rate at which precipitation and total condensate, respectively, are generated in the cloud volume. For the case when the amounts of water and ice within the cloud remain constant, the precipitation rate plus the evaporation rate, E, equals the condensation rate. Eq. 1 becomes

$$\varepsilon = 1/(1 + E/P) \quad . \; . \; . \; . \; . \; . \; . \; . \; . \quad (2)$$

For our present purpose we assume that the cloud is uniform along the barrier length and that liquid water directly over the barrier crest is evaporated downwind. Thus, the evaporation rate is expressed as $E = \int (LWC)_c u dz \simeq (LWC)_c \bar{u} H$, where $(LWC)_c$ is the liquid cloud water over the barrier crest, u is the cross-barrier wind speed, and H is the layer depth of cloud water; the precipitation rate is expressed as $P = \int I V_t dL \simeq \bar{I}\bar{V}_t L$, where I is the precipitation ice concentration at the cloud boundaries, V_t is the fall velocity, and L is the cross-barrier distance over which precipitation is falling. Also, the precipitation, p, measured at a

5.3.5 Analysis of seedability by use of cloudsonde data. Following a similar approach to the analysis of seedability as that for the analysis of airborne measurements and aircraft icing reports, the cloudsonde data collected during February and March, 1980 are utilized along with other relevant data. In particular SLWC, precipitation and their ratio (listed in Table 3 of Section 5.2.2) are plotted as a function of cross-barrier wind speed at 2700 m (9000 ft) and cloud top temperature in Figs. 24, 25, and 26, respectively.

It is found that at cloud top temperatures equal to or warmer than -22°C and at high cross-barrier wind speeds the supercooled liquid water concentration tends to be high. Precipitation tends to be highest at the cold cloud top temperatures. The ratios of supercooled liquid water to precipitation are such that high values occur in the warm cloud top temperature category and low values occur in the cold category. While there are only three data points in the cold category, they do fit the general pattern previously found in both the physical measurement program and the study utilizing aircraft icing reports.

Furthermore, it is noted that these measurements of supercooled liquid water were made primarily in the absence of heavy precipitation and in orographic type clouds. There was a purposeful attempt to collect data when seedability would be favorable. This is not to say there would have been a high yield of precipitation if seeding were done: most of cross-barrier wind speed, provided the seedability ratio is high. In such a case the yield is roughly proportional to the square of the cross-barrier flow. Consequently, we may expect nearly ten times more precipitation potential from seeding in a 15 m s^{-1} cross-barrier wind compared to seeding in a 5 m s^{-1} wind. Based upon data in Fig. 18, about 20 percent of the cases have high modification potential, i.e., cloud top temperatures -22°C or warmer and cross-barrier wind at mountaintop levels 10 m s^{-1} or greater. This percentage of high yield cases is again in general agreement with findings previously discussed. It is noted that with the addition of more detailed data than are presently available, some modification of the specific values concerning seedability ranges may be required. On the other hand the present analysis yields a consistent result derived from both research and operational data.

It is to be emphasized at this point that there is little concern about blowover of seeding effects with the higher winds as advocated herein for optimum seeding opportunity. First, it is noted that the supercooled water generated by the flow is typically at altitudes near mountaintop levels or a few hundred meters above. Second, artificial seeding is directed at these levels, and what happens at cloud <u>top</u> levels (Elliott et al. 1978; Vardiman and Moore 1978) is of lesser concern. Blowover from levels where supercooled water is being generated would require far higher cross-barrier winds than are normally observed.

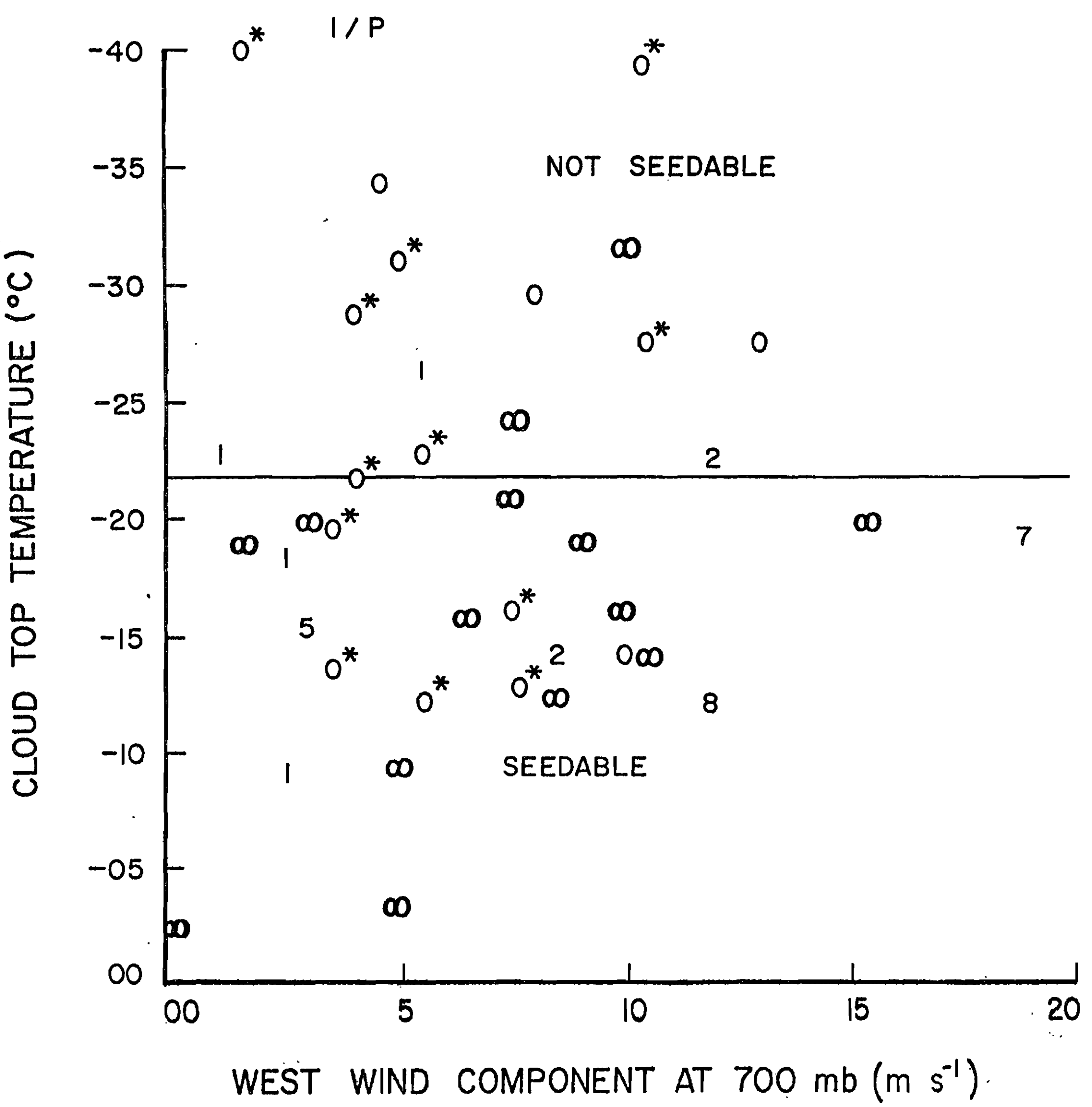

Fig. 23. Seedability ratios versus cloud top temperature and 700 mb cross-barrier wind speed. Note that 0* can be interpreted either as 0 or ∞ depending upon whether the cloud is primarily ice or supercooled water.

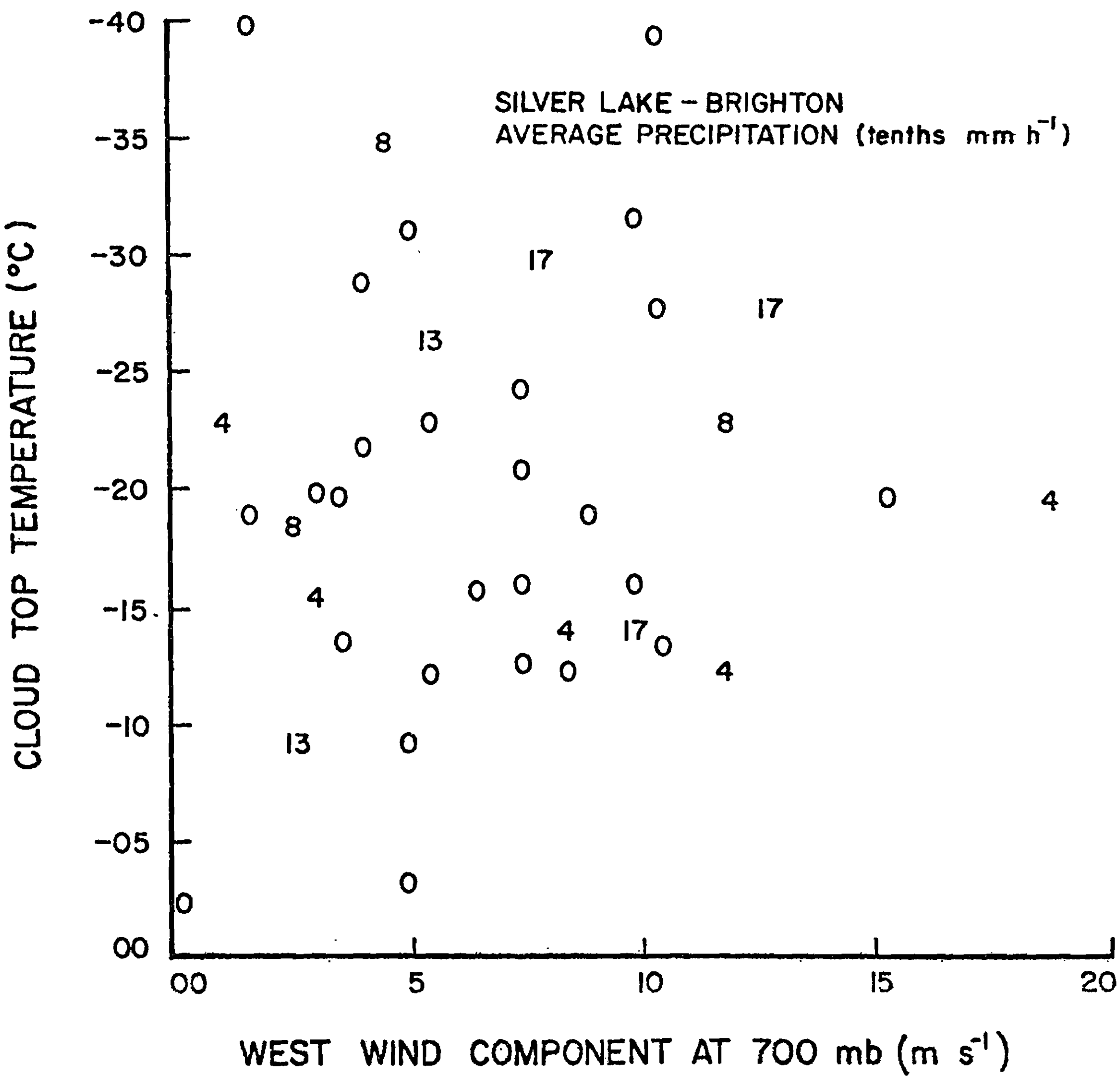

Fig. 22. Precipitation rate averaged over six hours at Silver Lake Brighton versus cloud top temperature and 700 mb cross-barrier wind speed.

and the supercooled water itself is roughly proportional to the wind speed, the flux of supercooled water is on an empirical basis approximately proportional to the square of the wind speed.

To assess seedability, the precipitation and seedability ratios are shown in Figs. 22 and 23, respectively. The seedability ratio shows a marked change on either side of a cloud top temperature of about -22°C. At warmer temperatures the ratio is high; at lower temperatures the ratio is low. The zeros marked with asterisks indicate neither icing nor precipitation was observed. However, either supercooled water or ice crystals could be present, depending upon the composition of the cloud.

Standardization of icing rates according to the number of daily takeoffs and landings at Salt Lake City resulted in very little change in the results. In particular, four of the values on Fig. 23 would be changed by 1 unit, e.g., 5 becomes 6; thus the air traffic is rather consistent within the days considered herein.

As indicated previously there are two considerations in establishing seeding opportunities. One is the seedability ratio, which is indicated by the total supercooled water compared to the precipitating ice; the other consideration is the total yield of precipitation if seeding were completely effective. The first quantity is determined solely by cloud top temperature. The second quantity is determined by the

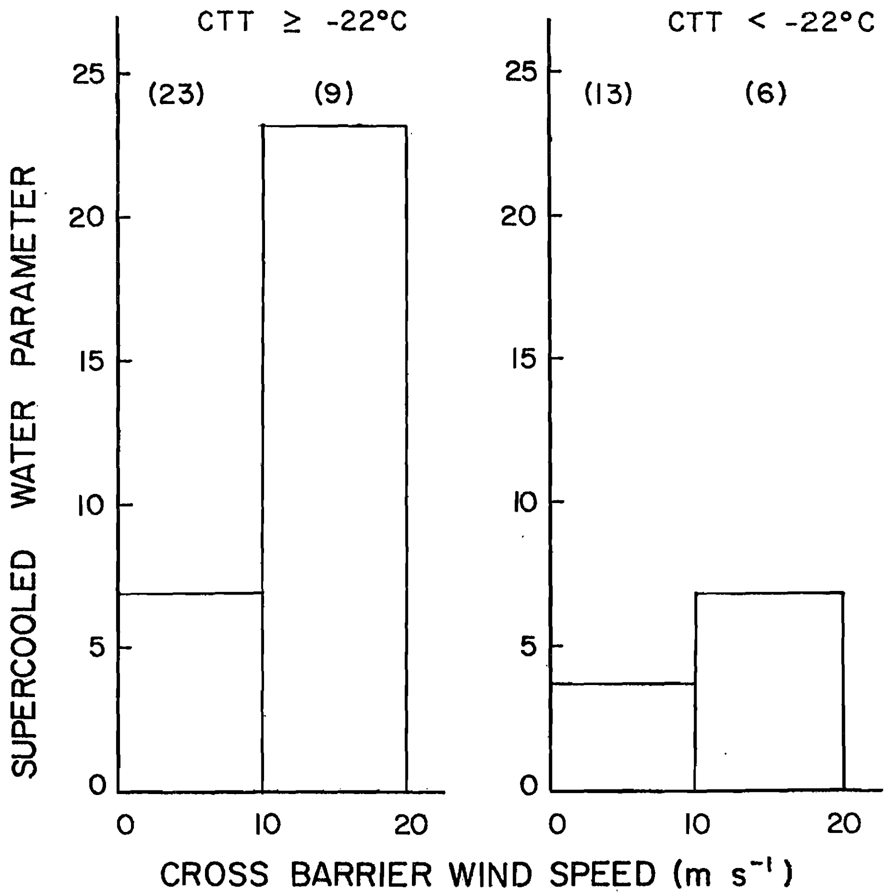

Fig. 21. Histograms of (average) supercooled water parameter versus cross-barrier wind speed for warm and cold cloud top temperatures.

This fact is further emphasized when the wind speed dependence is separated into warm and cold cloud top temperatures. As shown in Fig. 21 the supercooled water parameter is high when the cloud top temperature is warm and the wind speed is large. In the three remaining categories the supercooled water parameter is relatively low. The reason supercooled water itself is related to the wind speed is primarily that the vertical displacements increase as the wind speed increases. The least amount of supercooled water is found with cold cloud top temperatures and weak cross-barrier flow. These results apply to cases where deep convection is absent.

It has been suggested that another mechanism for the observation of higher liquid water content with high cross-barrier flow is that with higher winds there is less time for conversion of the water to ice. However, with cloud top temperatures warmer than -22°C it is doubtful that even at low velocities (5 m s^{-1}) there is sufficient time for conversion to ice except for very wide barriers. See Fig. 10 in Chappell and Johnson (1974). Thus, over the full range of observed wind speeds at warm temperatures there is insufficient time for substantial loss of supercooled water by conversion to ice. The increase in supercooled water with increasing vertical motion, or cross-barrier flow, is therefore attributed to an increased lifting distance with increased flow.

Because the flux of supercooled water over the barrier is the total supercooled water multiplied by the wind speed,

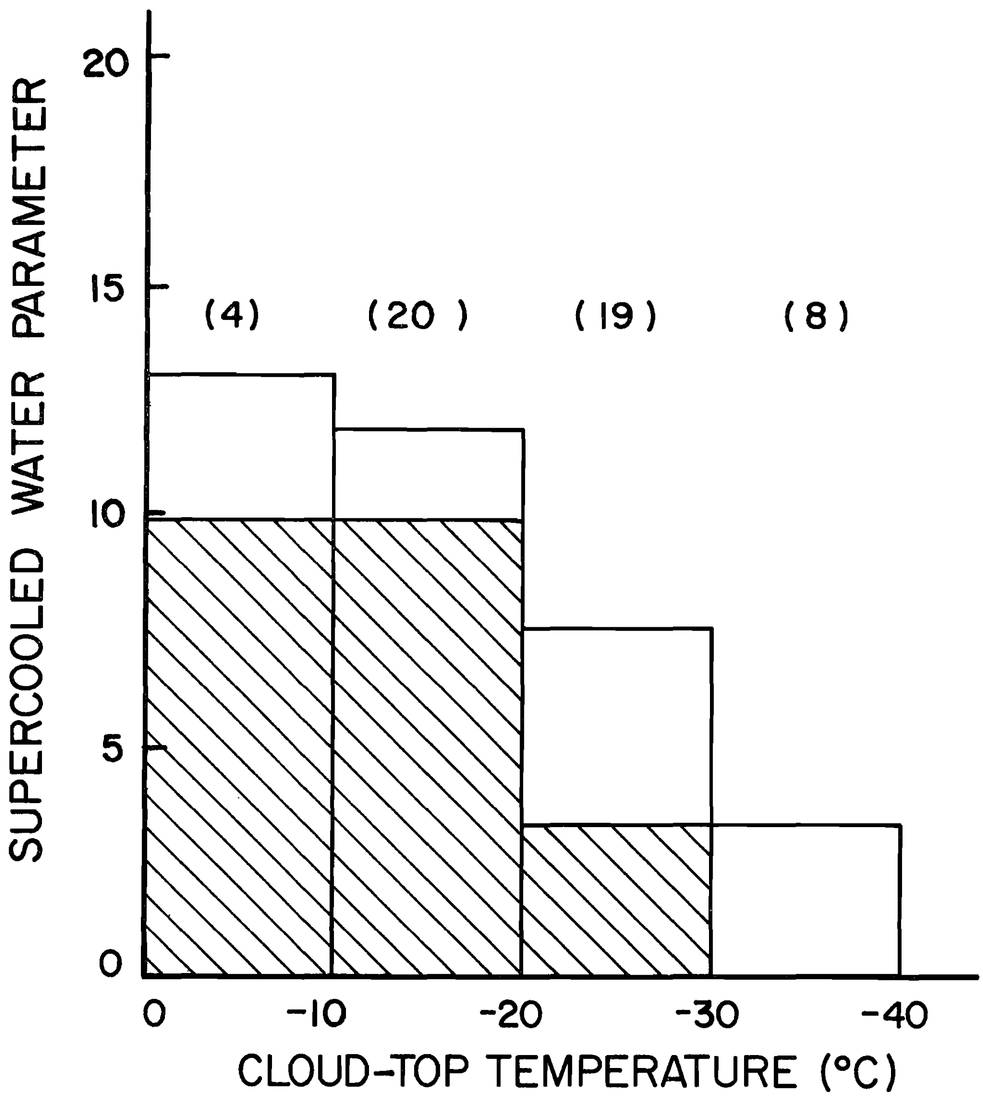

Fig. 20. Histogram of supercooled water parameter versus cloud top temperature. Hatched area refers to median values, full bar refers to average values. Numbers in parentheses are number of cases in each category.

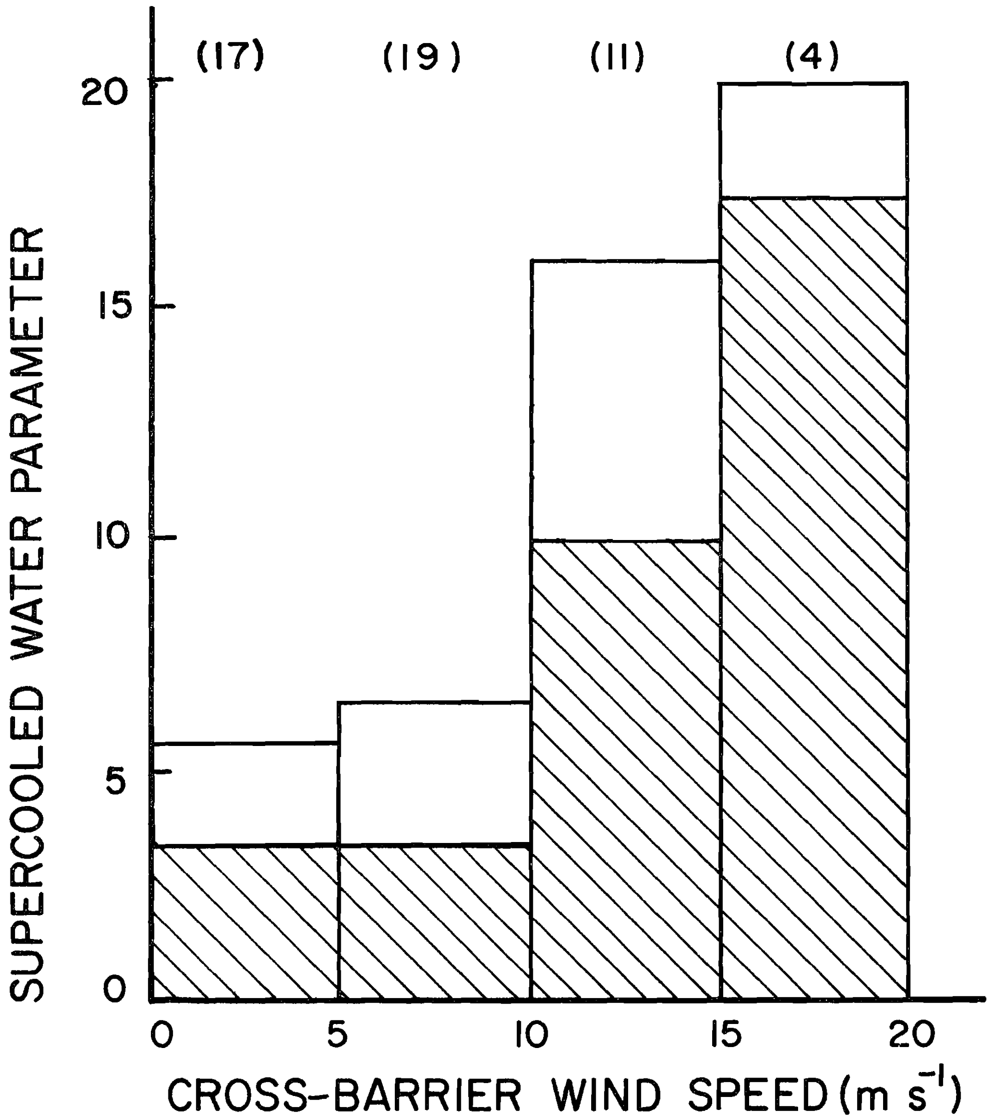

Fig. 19. Histogram of supercooled water parameter versus cross-barrier wind speed (700 mb level). Hatched area refers to median values, full bar refers to average values. Numbers in parentheses are number of cases in each category.

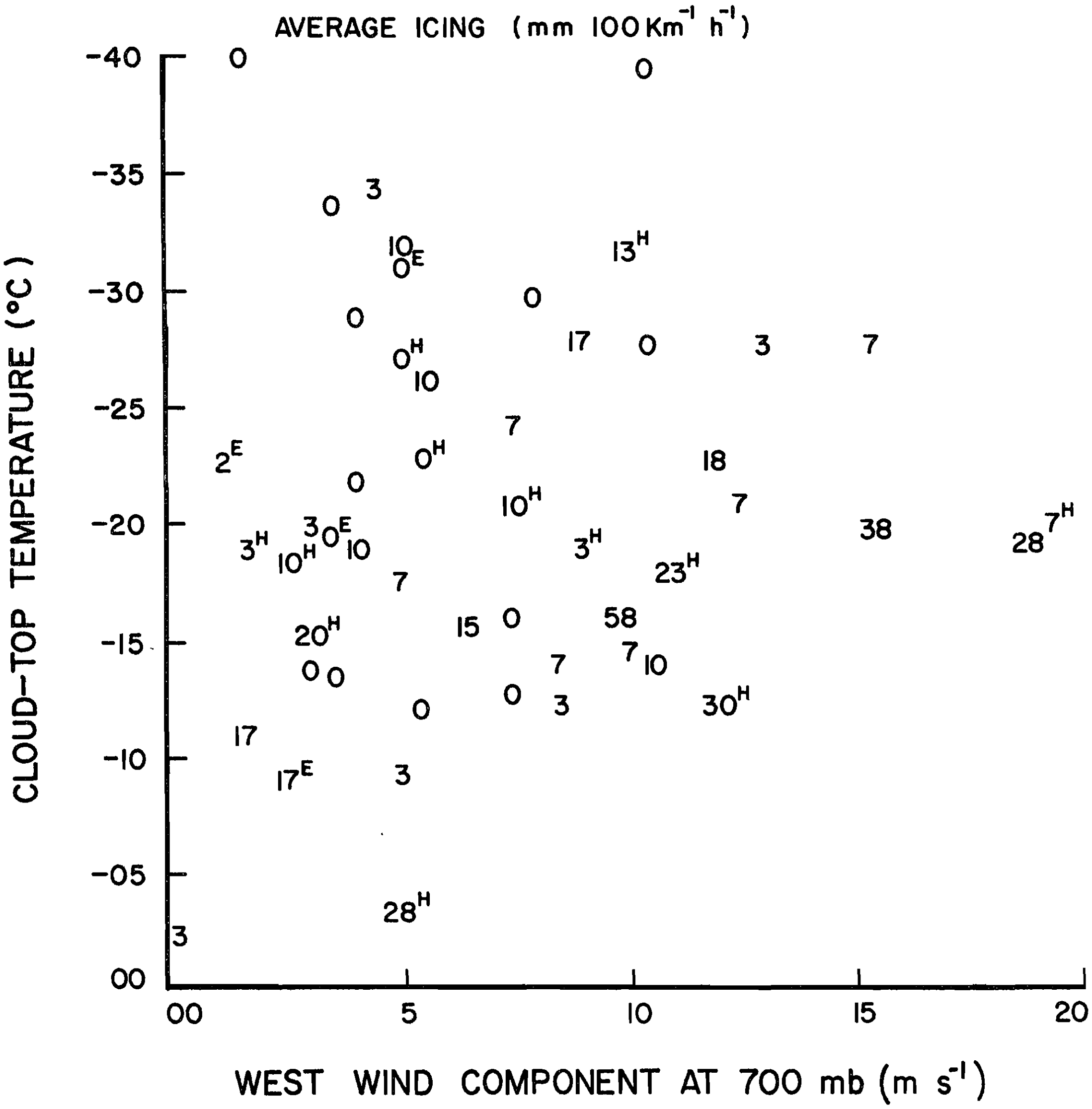

Fig. 18. Six-hour total aircraft icing expressed in mm per 100 km according to FAA definitions versus cloud top temperature and 700 mb cross-barrier wind speed. E indicates possible higher extension (lower cloud top temperature) of cloud. H indicates separate higher cloud layer above main layer.

percent r.h. criteria are used to find the base and top of a layer. A 50 mb separation is required for a separate layer, otherwise the cloud is treated as a single entity.

5.3.4 Results of preliminary test of seedability criteria. The results for aircraft icing are shown in Fig. 18. The cloud top temperatures used in this figure are those for the main layer based upon 100 percent r.h. If the cloud top temperature decreases by more than 3°C when a 90 percent r.h. criterion is used the data entered on the graph are marked with an "E," for possible extension of the cloud top. Clouds with a higher layer above are marked with an H. Also, all convection cases are omitted. However, the full data are available for inspection from Table 5; even when such data are included, the results are not substantially changed, though a more clear-cut distribution of supercooled water is obtained with convection cases omitted.

A histogram of supercooled water as indicated by aircraft icing is shown in Fig. 19 according to cross-barrier wind speed at 700 mb without regard for cloud top temperature. In Fig. 20 a histogram of supercooled water is shown according to cloud top temperature without regard for wind speed. In both of these figures a strong dependence of the supercooled water parameter with the other variable is evident. The greatest amount of supercooled water is found when the cloud top temperature is relatively warm and the cross-barrier flow at mountaintop is strong.

temperatures are found for both a 100 percent and a 90 percent relative humidity (r.h.) with respect to ice. If the cloud top temperature derived on the basis of a 90 percent r.h. is substantially different from one derived using 100 percent r.h., then such a case is specially identified. As will be shown later, in some instances even a substantial difference in cloud top temperature will have little effect on whether a cloud is seedable or not.

The representativeness in time and space of rawinsonde-determined cloud top temperatures is certainly affected by whether or not cellular convection is present. In the vicinity of cumulonimbus clouds, a sounding may or may not penetrate a deep cloud: the resulting cloud top temperature may therefore depart greatly from the coldest cloud top temperature. Furthermore, the occurrence of supercooled water in deep convection is related to the stage of development of the cloud rather than factors related to orographic flow. Consequently, cases with cumulonimbus clouds are identified in Table 5. To do this hourly and special reports from Salt Lake City during the six hour period centered on 0000 GMT are used. Any single report of CB or thunderstorm reported at or within observing distance of Salt Lake City results in a classification of convective activity. Twenty-two such cases were found.

The occurrence of multiple layers is found in a similar way as with the main cloud layer. Both 90 percent and 100

Table 5. Continued.

Date	I	P	I/P	U_{700}	Main Layer			Separated Higher Layer				Remarks
					CBT_{100}	CTT_{100}	CTT_{90}	CBT_{90}	CBT_{100}	CTT_{100}	CTT_{90}	
Jan 20	17	–	–	1.5	- 8.3	-10.8	-10.8	–	–	–	–	
24	0	–	–	3.5	-12.1	-34.1	-34.1	–	–	–	–	
25	2	4	1	1.0	- 7.0	-22.9	-40.0	–	–	–	–	
27	0	0	0*	5.5	-16.8	-23.0	-24.2	-30.1	-31.6	-35.0	-35.0	
28	0	0	0*	1.5	-17.5	-40.0	-40.0	–	–	–	–	
29	0	0	0*	4.0	-15.5	-29.2	-29.2	–	–	–	–	
31	0	0	0*	3.5	- 9.0	-19.7	-39.5	–	–	–	–	
Feb 1	3	0	∞	9.0	- 7.5	-19.0	-19.5	-31.0	-32.7	-39.8	-39.8	
2	0	0	0*	10.5	-14.5	-39.7	-40.0	–	–	–	–	
3	10	0	∞	7.5	-15.2	-21.0	-22.0	-37.0	–	–	-37.5	
4	3	0	∞	3.0	- 6.8	-20.0	-20.0	–	–	–	–	
5	10	0	∞	10.5	- 9.0	-14.0	-14.0	–	–	–	–	
6	58	0	∞	10.0	- 7.0	-16.0	-16.1	–	–	–	–	
7	38	0	∞	15.5	- 9.0	-19.8	-19.8	–	–	–	–	
8	3	0	∞	5.0	- 7.0	- 9.0	- 9.0	–	–	–	–	
13	18	8	2	12.0	- 5.3	-22.8	-22.8	–	–	–	–	
14	8	21	0	16.0	- 0.5	-37.5	-37.5	–	–	–	–	TSW
19	0	4	0	7.0	0.0	-28.7	-39.5	–	–	–	–	CB
21	0	17	0	8.0	- 1.8	-30.0	-36.8	–	–	–	–	
22	0	13	0	7.0	- 9.5	-24.8	-24.8	–	–	–	–	CB
23	3	4	1	4.5	- 2.5	-10.8	-14.2	–	–	–	–	TSW+
27	0	0	0*	5.5	- 5.0	-12.0	-12.1	–	–	–	–	
Mar 1	3	8	0	4.5	- 6.5	-34.8	-34.8	–	–	–	–	
2	0	0	0*	7.5	-11.8	-16.0	-16.7	–	–	–	–	
5	15	0	∞	6.5	- 5.3	-15.7	-16.2	–	–	–	–	
6	3	0	∞	0	- 1.1	- 2.0	- 1.7	–	–	–	–	
16	17	0	∞	2.5	- 8.5	-25.0	-25.0	–	–	–	–	CB
17	0	4	0	2.0	0.0	-36.9	-37.1	–	–	–	–	CB
19	3	0	∞	3.5	–	–	–	–	–	–	–	No cloud
21	0	4	0	0.5	- 4.0	-17.2	-18.0	-30.2	–	–	-36.0	CB
26	0	4	0	5.0	- 7.0	-24.0	-28.7	–	–	–	–	CB
27	23	30	1	17.5	- 6.2	-30.8	-32.9	–	–	–	–	CB
28	12	0	∞	0	-22.4	-35.5	-35.5	–	–	–	–	CB
29	3	8	0	6.0	- 5.7	-22.5	-23.2	–	–	–	–	CB
30	10	4	3	8.0	- 4.0	-21.8	-39.5	–	–	–	–	CB

Table 5. Tabulation of data (winter 1978-1979) for seedability verification. I is total aircraft icing rate (mm 100 km^{-1} h^{-1}); P is precipitation (mm h^{-1}); I/P is seedability ratio; U_{700} is cross-barrier wind at 700 mb (m s^{-1}); CBT and CTT refer to cloud base and cloud top temperatures, respectively; and subscripts refer to 90 percent or 100 percent relative humidity with respect to ice saturation.

Date	I	P	I/P	U_{700}	Main Layer			Separated Higher Layer				Remarks
					CBT_{100}	CTT_{100}	CTT_{90}	CBT_{90}	CBT_{100}	CTT_{100}	CTT_{90}	
Nov 1	2	0	∞	5.0	- 5.0	-18.0	-19.7	-	-	-	-	CB
2	3	17	0	13.0	1.7	-28.1	-28.1	-	-	-	-	
9	28	0	∞	5.0	0.0	- 3.0	- 3.0	-12.5	-	-	-14.7	
10	10	8	1	2.5	- 6.5	-18.4	-18.4	-27.3	-28.5	-29.1	-29.1	
11	17	13	1	2.5	- 0.5	- 8.7	-30.5	-	-	-	-	
12	3	17	0	10.0	0.2	-14.1	-23.0	-	-	-	-	TSW+
13	0	0	0*	3.5	- 8.0	-13.5	-13.7	-	-	-	-	
22	5	4	1	6.0	- 0.7	-18.7	-19.0	-	-	-	-	CB
25	3	0	∞	1.5	- 1.2	-19.0	-19.5	-25.0	-27.5	-34.8	-34.8	
26	20	4	5	3.0	- 5.2	-15.3	-15.5	-32.4	-34.0	-35.6	-35.7	
28	30	4	8	12.0	- 3.5	-12.0	-12.5	-30.0	-	-	-31.4	
29	7	4	2	8.5	- 0.6	-14.0	-14.0	-	-	-	-	
30	3	4	1	7.0	- 3.5	-28.4	-29.0	-	-	-	-	CB
Dec 1	3	8	0	4.0	- 4.5	-16.0	-16.0	-30.0	-	-	-35.5	CB
2	3	4	1	4.5	-16.7	-27.1	-28.5	-	-	-	-	CB
3	7	4	2	4.0	- 9.0	-25.0	-26.2	-	-	-	-	CB
4	28	4	7	19.0	- 1.1	-19.3	-20.2	-	-	-	-	
8	0	0	0*	4.0	-24.7	-22.0	-21.9	-	-	-	-	
9	3	0	∞	8.5	-10.5	-12.2	-12.5	-	-	-	-	
11	13	0	∞	10.0	-11.0	-32.0	-32.0	-	-	-	-	
17	10	13	1	5.5	- 4.4	-26.5	-26.5	-	-	-	-	
18	22	13	2	18.0	-18.0	-36.5	-36.5	-	-	-	-	CB
19	0	0	0*	5.0	- 8.0	-31.5	-45.0	-	-	-	-	
20	0	0	0*	7.5	-13.5	-12.5	-13.0	-	-	-	-	
21	7	17	0	10.0	- 8.5	-14.0	-14.1	-	-	-	-	
31	0	0	0*	10.5	-13.0	-28.0	-28.0	-	-	-	-	
Jan 2	7	0	∞	7.5	-13.2	-24.5	-24.5	-	-	-	-	
4	23	-	-	11.0	- 9.7	-18.0	-18.0	-30.5	-	-	-36.2	
5	0	-	-	3.0	- 8.5	-13.7	-13.7	-	-	-	-	
8	7	-	-	5.0	-15.3	-17.5	-16.8	-	-	-	-	
10	7	-	-	15.5	- 5.5	-28.0	-28.0	-	-	-	-	
11	7	-	-	19.5	- 2.0	-19.7	-20.4	-26.7	-26.9	-28.6	-28.6	
12	0	-	-	6.0	- 7.0	-20.1	-20.1	-	-	-	-	CB
13	0	-	-	8.0	- 8.8	-14.9	-14.9	-	-	-	-	CB
14	10	-	-	5.0	-10.0	-31.8	-31.8	-	-	-	-	
15	17	-	-	9.0	- 7.5	-28.2	-29.2	-34.8	-37.6	-40.5	-40.5	
17	7	-	-	12.5	- 8.2	-21.0	-24.2	-	-	-	-	
18	10	-	-	4.0	- 2.8	-19.1	-19.1	-	-	-	-	
19	0	-	-	5.0	- 9.5	-27.5	-27.5	-34.8	-36.5	-37.0	-37.0	

Table 4. Classification of aircraft icing reports.

Icing Rate	Abbreviation	Numerical Equivalent (mm 100 km^{-1})
Trace	T	10
Light	L	20
Light to Moderate	LM	30
Moderate	M	40
Moderate to Heavy	MH	60
Heavy	H	80

GMT Salt Lake City rawinsonde. Discussion of rawinsonde determined clouds and analysis of the data in Table 5 are presented in the next section.

5.3.3 Analysis of icing data. To derive cloud top temperatures from rawinsonde data, temperature and humidity data are utilized. In principle a cloud top temperature is found at the top of a layer in which the humidity is equal to or exceeds ice saturation. However, to apply this principle several factors must be considered. These are 1) the accuracy of the data, 2) representativeness of the data, and 3) the presence of multiple layers.

Prior to about 1972, U.S. rawinsonde humidity data were grossly in error during daytime. Since then a new design of the rawinsonde unit has resulted in much improved accuracy (e.g., Friedman 1972). However, small errors in marginal cloud conditions could lead to a substantial error in cloud top temperature. To address this uncertainty cloud top

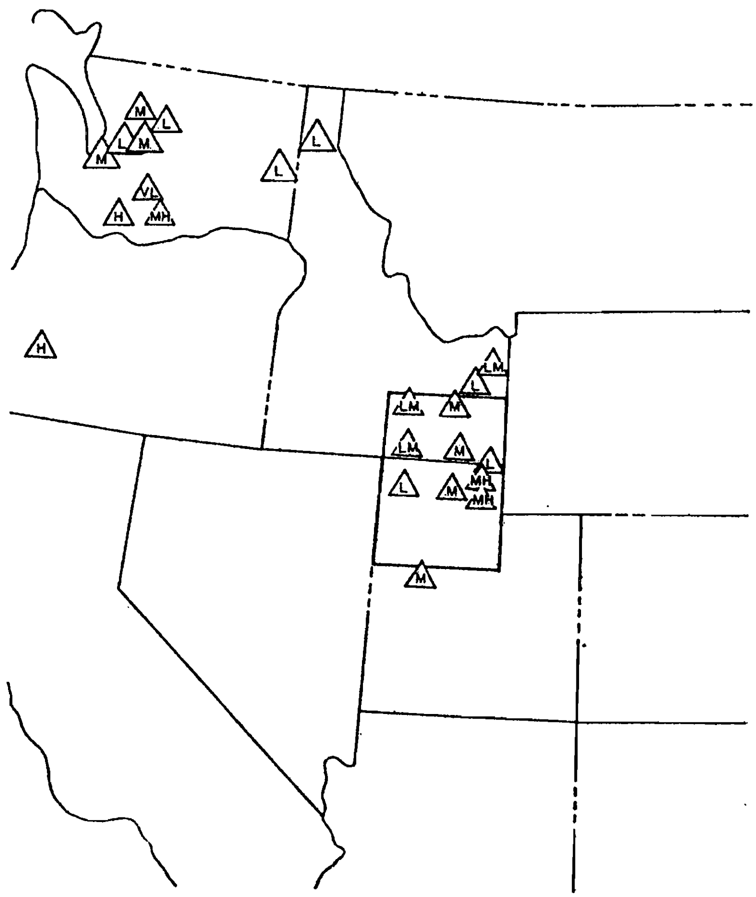

Fig. 17. Chart of icing reports 1400-2000 MST 6 Feb., 1979. Area in N. Utah and S. E. Idaho for obtaining aircraft icing reports also shown. See Table 4 for icing definitions.

In view of the foregoing, an area in the vicinity of N. Utah has been selected for obtaining aircraft icing reports to be used in the analysis. The area was chosen as small as possible for suitable representativeness, but large enough to obtain adequate sample sizes. For each day during winter period, November 1978 through March 1979, aircraft icing reports were tabulated for a period three hours before and three hours after the 0000 GMT Salt Lake City rawinsonde. The 1200 GMT soundings were not evaluated because there are very few aircraft reports at that time. A chart of aircraft icing reports in a highly seedable situation is shown for the six hour period on 6 February, 1979 in Fig. 17.

In processing the aircraft reports a standard method was adopted to quantify them. First, the icing rate designation for an individual report was established according to Federal Aviation Administration guidelines. These are listed in Table 4 (in metric units). Next, the icing rates were summed for all reports within the designated area and within the six hour period, so one value per day is found. All icing reports were quantified and an overall sum obtained for each six hour period, prior to any other data analysis.

Then the 700 mb wind, precipitation at Silver Lake Brighton over the same six hour period and cloud temperatures were tabulated; the relevant data are listed in Table 5. In this table, all dates are listed when either aircraft icing is reported or a cloud is present as determined by the 0000

At this point, it is noted that the present hypothesis is in conflict with the so-called "barrier trajectory index" or "blowover index" concepts as proposed by Elliott et al. (1978) and applied to past experiments by Vardiman and Moore (1978). Whereas these indices are related in part to conditions at cloud top, our data indicate that the production of supercooled water is closely associated with vertical air motion which in turn is found primarily at or near mountaintop levels. Should this supercooled water be effectively seeded, the resulting precipitation could be expected to fall on the mountain, even in most observed winds considered excessively strong according to the "barrier trajectory index."

5.3.2 Data for preliminary verification of hypothesis. As a preliminary demonstration of the merit of the foregoing criteria, we have found similar relationships using more readily available National Weather Service data. For supercooled water concentrations aircraft icing reports are used; for vertical motion, it is assumed the updraft speed is proportional to the mountaintop wind normal to the barrier. The cloud base and tops are derived from standard NWS rawinsondes. Of the various regularly reporting NWS rawinsonde stations, the one situated at Salt Lake City is in a unique location particularly well suited for the present study. These rawinsonde observations are made only about 20 km upwind of a mountain range with peaks rising about 2500 m above the rawinsonde release point.

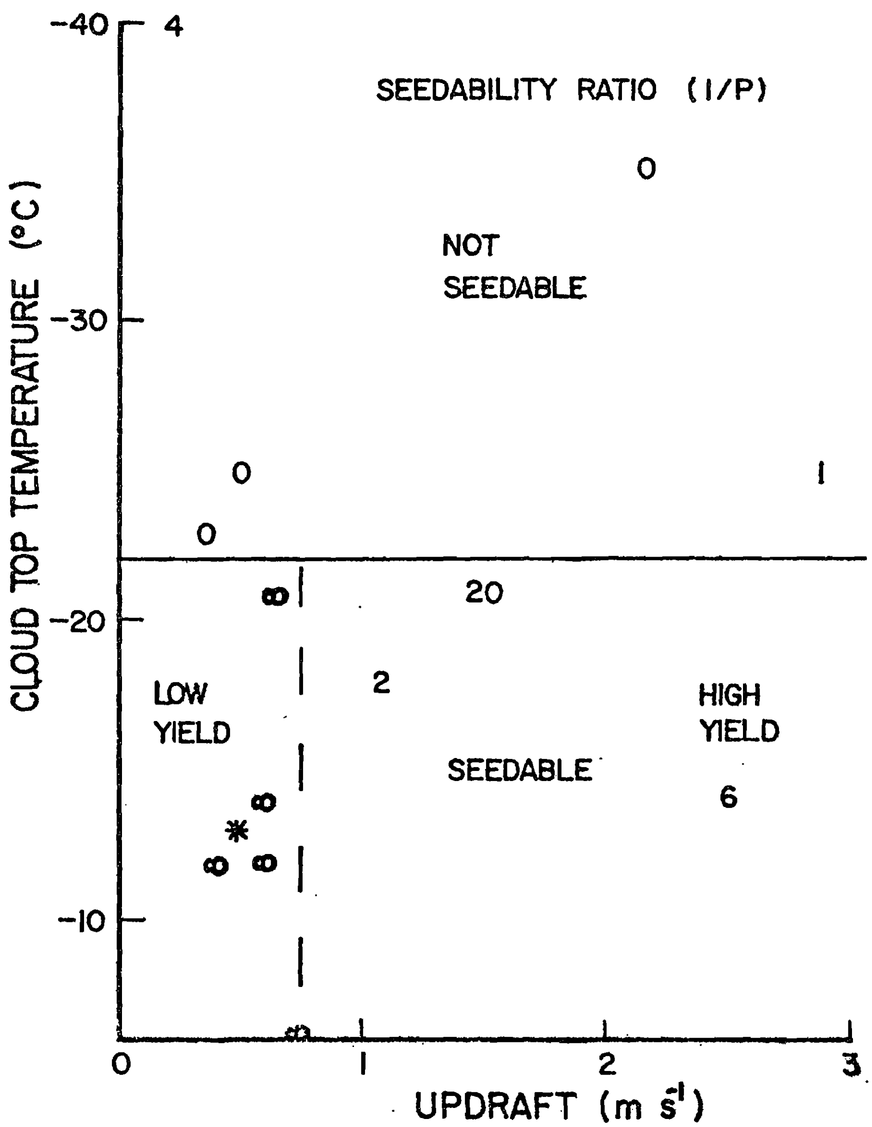

Fig. 16. Seedability ratios for available FY78 and 79 airborne and ground based data.

fixed horizontal level is $3.6IV_t$ (mm h^{-1}). From these expressions we find

$$\varepsilon = 1/(1 + A_1(LWC)_c/I) \quad . \; . \; . \; . \; . \; . \; . \; . \quad (3)$$

or

$$\varepsilon = 1/(1 + A_2(LWC)_c/p) \quad . \; . \; . \; . \; . \; . \; . \; . \quad (4)$$

where $A_1 = UH/(V_tL)$ and $A_2 = 3.6UH/L$. Either (3) or (4) may be used to obtain estimates of the precipitation efficiency.

To quantify seedability we utilize the ratio $(LWC)_c/I$ in (3) or $(LWC)_c/p$ in (4), either of which we identify as a "seedability ratio." So, if there is little supercooled water and substantial precipitation the seedability ratio (SR) will approach zero. On the other hand if the supercooled water concentration is high (over the barrier crest) and there is little or no precipitation then the ratio will approach infinity. Depending upon the availability of data some measure of the supercooled water concentration and precipitation is required to evaluate SR. In our case we use supercooled water concentrations derived from measured icing rates and hourly precipitation rates at Smithfield Canyon.

The seedability ratios for available FY78 and FY79 data are shown in Fig. 16. From these data it appears that with cloud top temperatures of -22°C and warmer there is a seeding potential. However, it is pointed out that even with an infinite SR the actual amount of increase from seeding may be small.

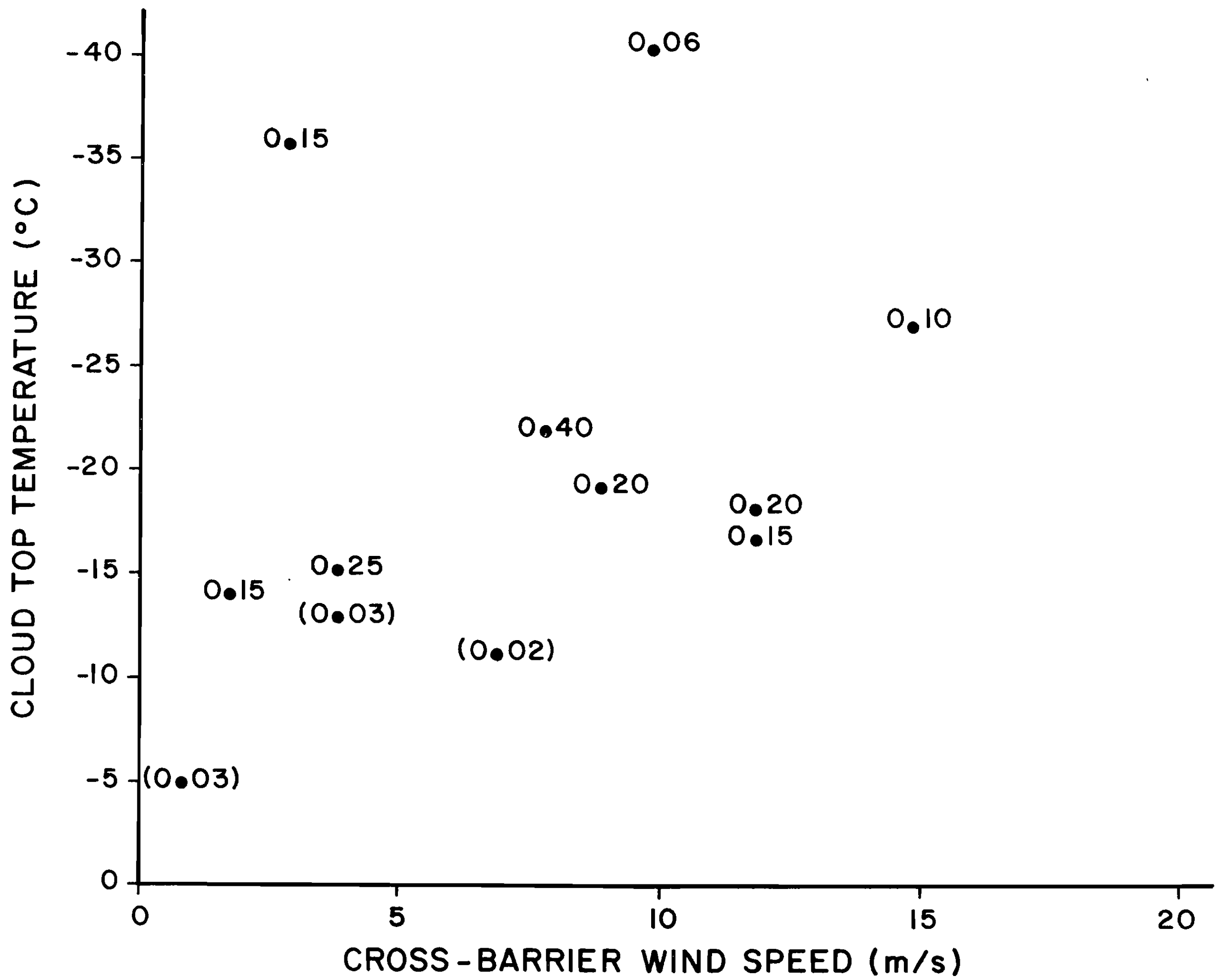

Fig. 24. Supercooled liquid water (g m^{-3}) measured by cloud-sondes (FY80) versus cloud top temperature and 2700 m (9000 ft) cross-barrier wind speed.

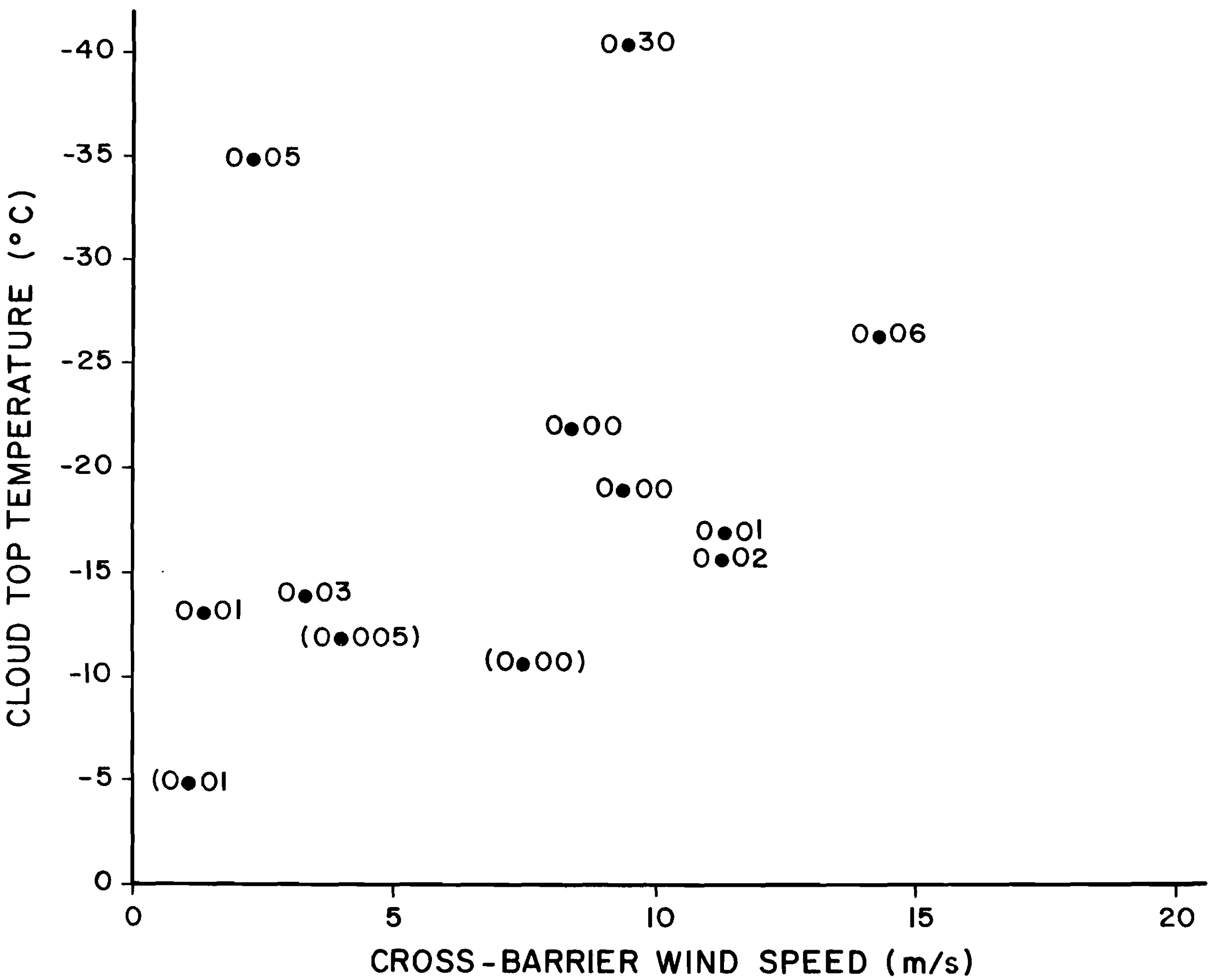

Fig. 25. Precipitation rate (cm h^{-1}) at Smithfield Canyon versus cloud top temperature and 2700 m (9000 ft) cross-barrier wind speed.

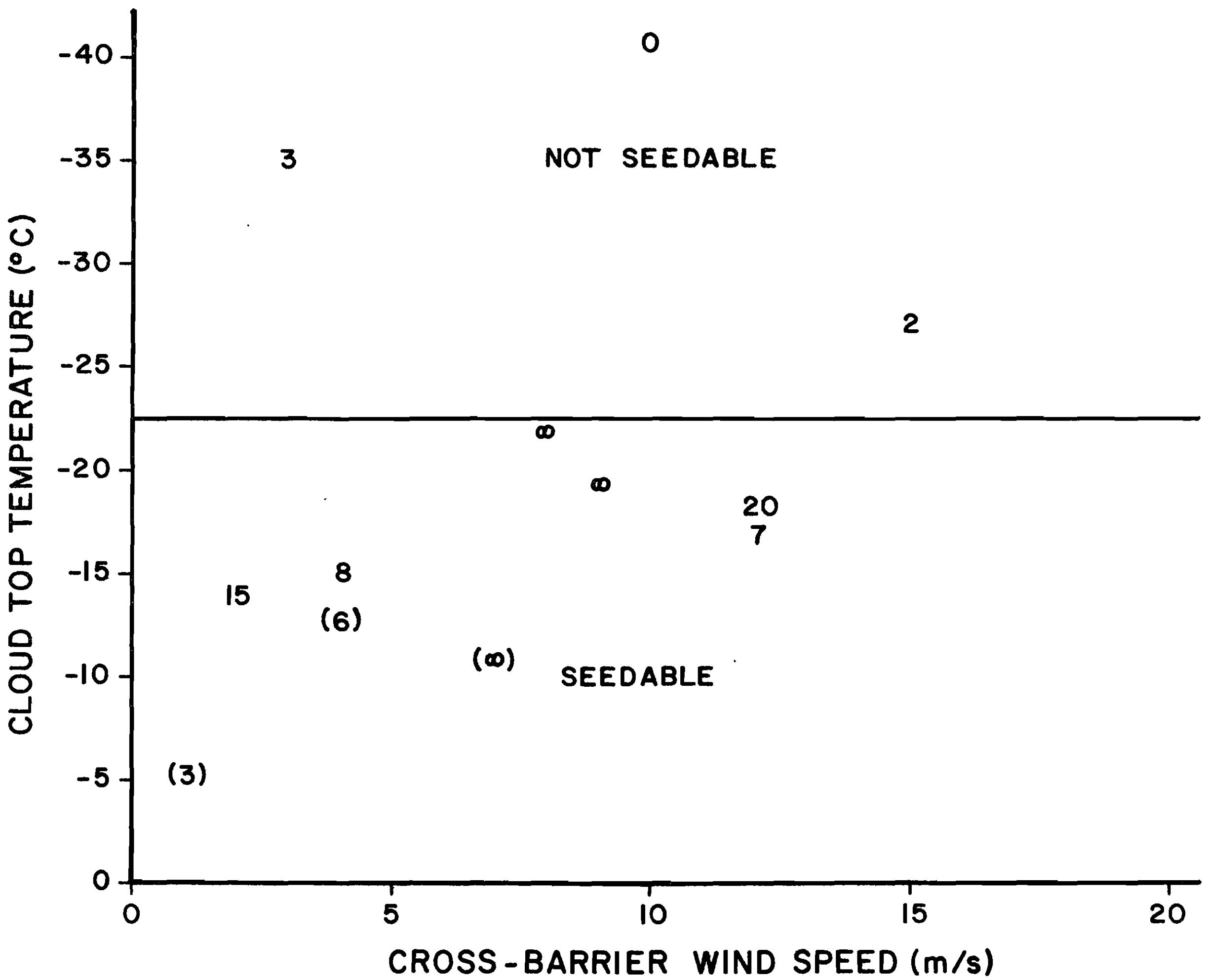

Fig. 26. Seedability ratios versus cloud top temperature and 2700 m (9000 ft) cross-barrier wind speed.

the clouds were relatively thin. Clouds with a temperature difference between cloud base and cloud top of 3°C or less are indicated by parentheses on Fig. 26. Precipitation associated with these cases is very low, and probably close to or below the detection limit of the weighing gage system.

Thus, it would be appropriate to place greatest emphasis on the remaining cases. The remaining pattern of seedability as a function of cloud top temperature becomes quite clear: at cold cloud top temperatures there is little potential for precipitation augmentation; at warm cloud top temperatures the precipitation efficiency is low; and if both the supercooled liquid water concentration and cross-barrier wind speed are high, a substantial precipitation augmentation potential exists.

5.3.6 Summary of seedability analysis. Analysis of supercooled water concentrations and precipitation as functions of cloud top temperature and orographic updraft speeds indicates that seedability is marked (in N. Utah) by cloud top temperatures -22°C or warmer, but below 0°C, and updraft speeds of 1 m s^{-1} or greater (Hill 1979). This hypothesis is further substantiated in the present work by aircraft icing reports as a substitute for supercooled water concentrations and cross-barrier flow as a substitute for vertical motion. Still further verification of these criteria are obtained by use of the new cloudsonde measurements of supercooled liquid water.

Within the suitable cloud top temperature range, the potential precipitation yield increases as square of the cross-barrier wind speed increases. About 20 percent of winter orographic clouds offer such high potential.

According to our present seedability criteria, we would expect high seedability to be associated with a) post frontal conditions, where i) the cross-barrier flow is strong, ii) high level subsidence is occurring, and iii) moisture is still high at mountaintop levels, and b) weak low level moisture systems with strong airflow (and perhaps weak subsidence aloft). Both types of seedable conditions are very similar and may be distinguished only by the presence or absence of a prior cyclonic system. We believe, as a corollary to the present hypothesis, that excepting possibly for convection, there is generally an absence of seeding opportunities in other cloud systems, especially well developed cyclonic storms.

6.0 CONCLUSIONS AND RECOMMENDATIONS

6.1 Conclusions

The following conclusions are derived from the foregoing research:

1. A cloudsonde instrument has been developed to measure vertical profiles of supercooled liquid water (and vertical motion). The first season's data indicate the supercooled liquid water measurements are very useful in assessing seeding potential.

2. The development of a dual frequency radiometer is underway and may be expected to play an important role in research on winter orographic cloud seeding.

3. Measurements of supercooled liquid water by the Johnson-Williams device are subject to large errors in winter orographic clouds, and the use of a Rosemount icing rate meter gives more reliable data.

4. Aircraft icing reports may be effectively used to provide information on cloud seedability, and these data reinforce previous findings. Briefly, it is found that a substantial cloud seeding opportunity is present if the cloud top temperature just upwind of the barrier is warmer than about -22°C and the cross-barrier wind speed is greater than 8 (or 10) m s^{-1}.

6.2 Recommendations

The following recommendations are derived from the foregoing work:

1. Further development, testing and operation of the cloudsonde units are strongly recommended. It is likely that data obtained from these soundings will provide heretofore unavailable information critical to the development of cloud seeding technology.

2. Completion and operation of the dual frequency radiometer (for continuous measurement of supercooled liquid water --vertically integrated) is also strongly recommended. These data will also provide previously unavailable measurements.

3. Collection of additional data for assessing cloud seeding opportunity recognition is recommended. These data include cloud top temperature, vertical motion, cross-barrier wind speed, supercooled liquid water and precipitation.

REFERENCES

Chappell, C. F., and F. L. Johnson, 1974: Potential for snow augmentation in cold orographic clouds. J. Appl. Meteor., 13, 374-382.

Elliott, R. D., R. W. Shaffer, A. Court, and J. F. Hannaford, 1978: Randomized cloud seeding in the San Juan Mountains, Colorado. J. Appl. Meteor., 17, 1298-1318.

Friedman, M., 1972: A new radiosonde case: The problem and the solution. Bull. Amer. Meteor. Soc., 53, 884-887.

Guiraud, F. O., J. Howard, and D. C. Hogg, 1979: A dual-channel microwave radiometer for measurement of precipitable water vapor and liquid. I.E.E.E. Trans. Geosc. Electron., GE-17, 129-136.

Hill, G. E., 1979: Research on increased winter orographic precipitation by cloud seeding (FY1979): Development of cloud seedability criteria. Atmospheric Water Resources Series UWRL/A-79/01, Utah Water Research Laboratory, Utah State University, Logan, Utah. 73 pp.

Hill, G. E., and D. S. Woffinden, 1980: A balloonborne instrument for the measurement of vertical profiles of supercooled liquid water concentration. J. Appl. Meteor., 19. 8 pp.

Langmuir I., and K. B. Blodgett, 1946: A mathematical investigation of water droplet trajectories. Army Air Forces Tech. Rep. No. 5418. 68 pp.

Ludlam, F. H., 1951: The best economy of a rimed cylinder. Quart. J. Roy. Meteor. Soc., 77, 663-666.

Neel, C. B., Jr., and C. P. Steinmetz, 1952: The calculated and measured performance characteristics of a heated-wire liquid-water content meter for measuring icing severity. NACA Tech. Note 2615. 37 pp.

Vardiman, L., and J. A. Moore, 1978: Generalized criteria for seeding winter orographic clouds. J. Appl. Meteor., 17, 1769-1777.